

Prospects for new physics in $\tau \rightarrow l\mu\mu$ at current and future colliders

Chris Hays,^a Manimala Mitra,^{b,c} Michael Spannowsky^c and Philip Waite^c

^a*Department of Physics, Oxford University,
Keble Road, Oxford, OX1 3RH, U.K.*

^b*Department of Physics,
Indian Institute of Science Education and Research Mohali (IISER Mohali),
Sector 81, SAS Nagar, Manauli 140306, India*

^c*Institute for Particle Physics Phenomenology, Department of Physics, Durham University,
South Road, Durham, DH1 3LE, U.K.*

E-mail: chris.hays@physics.ox.ac.uk, manimala@iisermohali.ac.in,
michael.spannowsky@durham.ac.uk, p.a.waite@durham.ac.uk

ABSTRACT: The discovery of lepton flavour violating interactions will be striking evidence for physics beyond the Standard Model. Focusing on the three decays $\tau^\mp \rightarrow \mu^\pm \mu^\mp \mu^\mp$, $\tau^\mp \rightarrow e^\pm \mu^\mp \mu^\mp$ and $\tau^\mp \rightarrow e^\mp \mu^\mp \mu^\pm$, we evaluate the discovery potential of current and future high-energy colliders to probe lepton flavour violation in the τ sector. Based on this potential we determine the expected constraints on parameters of new physics in the context of the Type-II Seesaw Model, the Left-Right Symmetric Model, and the Minimal Supersymmetric Standard Model. The existing and ongoing 13 TeV run of the Large Hadron Collider has the potential to produce constraints that outperform the existing e^+e^- collider limits for the $\tau^\mp \rightarrow \mu^\pm \mu^\mp \mu^\mp$ decay and achieve a branching fraction limit of $\lesssim 10^{-8}$. With a future circular e^+e^- collider, constraints on the $\tau \rightarrow l\mu\mu$ branching fractions could reach as low as a few times 10^{-12} .

KEYWORDS: Beyond Standard Model, Gauge Symmetry, Higgs Physics, Neutrino Physics

ARXIV EPRINT: [1701.00870](https://arxiv.org/abs/1701.00870)

Contents

1	Introduction	1
2	Experimental limits	2
2.1	Current limits	3
2.2	Future limits	4
3	Standard Model extensions with lepton flavour violating interactions	6
3.1	Type-II Seesaw Model	6
3.2	Left-Right Symmetric Model	10
3.2.1	Neutrino mass	11
3.2.2	Higgs mass	12
3.2.3	Limits from the LFV branching ratios	13
3.3	Minimal Supersymmetric Standard Model	16
4	Conclusions	18

1 Introduction

In the Standard Model, the Yukawa couplings break the global flavour group G_F explicitly to an accidental subgroup $G_F \equiv \text{SU}(3)^5 \rightarrow \text{U}(1)_B \times \text{U}(1)_{L_1} \times \text{U}(1)_{L_2} \times \text{U}(1)_{L_3}$. Hence, the model exhibits flavour conservation to all orders in perturbation theory that prohibits any process where charged lepton flavour is not conserved. Despite the immense success of the Standard Model (SM), it does not serve as an adequate description of nature due to its inability to explain the experimentally observed non-zero neutrino masses and mixings, the radiative stability of the Higgs mass, and the existence of dark matter, for which beyond the Standard Model (BSM) descriptions are necessary. Going beyond the SM, the models that successfully explain the above problems often introduce lepton flavour violation (LFV) either at tree-level or via loop-induced processes.

A selection of the interesting models that provide large lepton flavour violation are the various seesaw models [1–15], the Left-Right Symmetric Model (LRSM) [16–19], and the Minimal Supersymmetric Standard Model (MSSM) [20–22]. In the seesaw framework, small Majorana masses of the light neutrinos are generated from the dimension-5 operator $LLHH/\Lambda$ [23, 24] through electroweak symmetry breaking. The high-scale theory contains a plethora of new particles, such as an extended neutrino sector for the Type-I [1–5], Type-III [10] and inverse seesaw [11–15] models, and an extended scalar sector for the Type-II Seesaw Model [6, 7]. In the LRSM [16–19], the model contains both extended neutrino and Higgs sectors, and the light neutrino masses are generated via a combination of Type-I and Type-II seesaw mechanisms. The non-trivial interactions of the heavy neutrinos or

scalars with the SM charged leptons allow for a priori unsuppressed LFV interactions in these theories. In the MSSM, the large LFV is introduced by the non-diagonal slepton mass matrices. The large LFV rates of these new particles can be tested at present and future colliders. Hence, experimental evidence for a non-zero LFV rate will serve as striking evidence for the existence of physics beyond the Standard Model.

The existing experimental constraints for LFV in transitions between the first and second generations are quite tight: $\text{BR}(\mu \rightarrow e\gamma) \leq 5.7 \times 10^{-13}$ at 90% confidence level (C.L.) as reported by MEG [25, 26], and $\text{BR}(\mu^\mp \rightarrow e^\pm e^\mp e^\mp) \leq 10^{-12}$ at 90% C.L. [26, 27]. Lepton flavour violation in τ lepton decays is much less constrained: $\text{BR}(\tau \rightarrow lll) \lesssim 10^{-8}$ at 90% C.L. [26], allowing for rather large flavour violating couplings. Considering low-energy models, one can avoid the stringent constraints from the LFV processes involving the first and second generations. The recent excess in $h \rightarrow \tau\mu$ reported by CMS [28], as well as a smaller excess by ATLAS [29], spurred further interest in collider studies of flavour-changing neutral interactions in decays of the Higgs boson and the τ lepton [30–36]. Experimental limits from the Belle and BaBar experiments at the flavour factories are currently the most stringent, requiring the branching ratio for the $\tau^\mp \rightarrow \mu^\pm \mu^\mp \mu^\mp$ decay to be less than 2.1×10^{-8} at 90% C.L. Similar exclusion limits are obtained for the $\tau^\mp \rightarrow e^\pm \mu^\mp \mu^\mp$ and $\tau^\mp \rightarrow e^\mp \mu^\mp \mu^\pm$ modes. A recent search from the LHCb experiment produced a competitive constraint for the $\tau^\mp \rightarrow \mu^\pm \mu^\mp \mu^\mp$ decay, with the limit a factor of two larger than the constraints from Belle, $\text{BR}(\tau^\mp \rightarrow \mu^\pm \mu^\mp \mu^\mp) \leq 4.6 \times 10^{-8}$ at 90% C.L. The recent bound from ATLAS is one order of magnitude smaller, though current and future 13 TeV data sets from ATLAS and CMS can significantly extend this sensitivity to $\text{BR}(\tau^\mp \rightarrow \mu^\pm \mu^\mp \mu^\mp) \sim 10^{-9}$. The Belle-II experiment and a possible future circular collider will be sensitive to even lower branching ratios, $\sim 10^{-10}$ and $\sim 10^{-12}$, respectively.

In this work we analyse LFV in the τ sector, focusing on the decay modes $\tau^\mp \rightarrow \mu^\pm \mu^\mp \mu^\mp$, $\tau^\mp \rightarrow e^\pm \mu^\mp \mu^\mp$, and $\tau^\mp \rightarrow e^\mp \mu^\mp \mu^\pm$. We consider the potential of both e^+e^- and hadron colliders, including future circular colliders, in searching for LFV in τ lepton decays. Using the expected constraints we derive the sensitivity reach for three BSM models: the Type-II Seesaw Model, the LRSM, and the MSSM.

The rest of the paper is organised as follows: in section 2, we discuss current and future limits from flavour factories and high-energy colliders on rare flavour violating τ decays. In section 3, we test popular and widely studied extensions of the SM, such as the Type-II Seesaw Model, the LRSM and the MSSM, using the limits collected in section 2. While the Type-II Seesaw Model and the LRSM induce tree-level LFV interactions, LFV processes are generically loop suppressed in the MSSM. Nonetheless, particularly for the former two models [37–41] but also for the MSSM [42–44], LFV has become a litmus test, excluding large areas of the parameter space. Finally, in section 4, we present our conclusions.

2 Experimental limits

We review present and future collider constraints on the processes $\tau^\mp \rightarrow \mu^\pm \mu^\mp \mu^\mp$, $\tau^\mp \rightarrow e^\pm \mu^\mp \mu^\mp$ and $\tau^\mp \rightarrow e^\mp \mu^\mp \mu^\pm$. Limits on τ lepton decays to three charged leptons have been obtained at both e^+e^- and hadron colliders, with the B-factories currently giv-

ing the most stringent limits. However, the data from the LHC run at $\sqrt{s} = 13$ TeV could result in stronger $\tau^\mp \rightarrow \mu^\pm \mu^\mp \mu^\mp$ limits than those from B-factories. In the long run, the upgraded KEKB e^+e^- collider and a potential future circular e^+e^- collider are expected to provide the greatest sensitivity to these processes.

2.1 Current limits

The Belle and BaBar experiments probe the six possible combinations of τ lepton decays to three charged leptons using e^+e^- integrated luminosities of 782 fb^{-1} [45] and 468 fb^{-1} [46], respectively, representing nearly the complete available data sets. The $\tau^+\tau^-$ cross section is 0.919 nb , giving 720 (430) million τ lepton pairs in the Belle (BaBar) data set. Events are selected at Belle by requiring one identified τ lepton decay (the “tag” τ lepton) and searching for a lepton flavour violating τ lepton decay (the “signal” τ lepton). The background is very low after a basic selection and is primarily due to $\tau^+\tau^-$ production or quark-antiquark production with misidentified leptons for the $\tau^\mp \rightarrow \mu^\pm \mu^\mp \mu^\mp$ and $\tau^\mp \rightarrow e^\pm \mu^\mp \mu^\mp$ searches. For the $\tau^\mp \rightarrow e^\mp \mu^\mp \mu^\pm$ decay the main contribution is $\gamma\gamma \rightarrow \mu^+\mu^-$ with a scattered electron. In the $\tau^\mp \rightarrow \mu^\pm \mu^\mp \mu^\mp$ case, an additional background rejection is applied using the missing momentum and missing mass-squared in the event. This decreases the efficiency of the selection to 7.6% (the efficiency of the $\tau^\mp \rightarrow e^\pm \mu^\mp \mu^\mp$ selection is 10.1%). The expected background, estimated from data, is 0.02–0.13 events. No events are observed and the 90% C.L. upper limits on the branching fractions are 2.1×10^{-8} , 1.7×10^{-8} , and 2.7×10^{-8} for $\tau^\mp \rightarrow \mu^\pm \mu^\mp \mu^\mp$, $\tau^\mp \rightarrow e^\pm \mu^\mp \mu^\mp$, and $\tau^\mp \rightarrow e^\mp \mu^\mp \mu^\pm$ respectively. The corresponding limits from BaBar are 3.3×10^{-8} , 2.6×10^{-8} , and 3.2×10^{-8} .

The LHCb experiment has searched for $\tau^\mp \rightarrow \mu^\pm \mu^\mp \mu^\mp$ in 3 fb^{-1} of pp collision data at centre-of-mass energies of 7 and 8 TeV [47]. The production of τ leptons at the LHC occurs predominantly through the decays of heavy quarks, with an inclusive cross section of approximately $85 \mu\text{b}$. The τ lepton yield is normalised using the $D_s \rightarrow \phi(\mu\mu)\pi$ decay, the relative branching fractions for $D_s \rightarrow \phi(\mu\mu)\pi$ and $D_s \rightarrow \tau\nu$, and the fraction of τ leptons that are produced via $D_s \rightarrow \tau\nu$. Backgrounds from $D_s \rightarrow \eta(\mu\mu\gamma)\mu\nu$ decays motivate a fit of the three-muon mass distribution in 30 (35) bins of particle-identification and geometric-event classifiers in $\sqrt{s} = 7$ (8) TeV data. The fit describes the background as an exponential distribution in the mass range (1600–1950) MeV, excluding the signal window of ± 30 MeV around the τ lepton mass. The observed yields in the signal region are consistent with the background and range from 0 to 39 events, with the highest yields present in bins of the particle identification classifier where the misidentification backgrounds $D_{(s)} \rightarrow K\pi\pi$ and $D_{(s)} \rightarrow \pi\pi\pi$ are significant. These bins are excluded when deriving the 90% C.L. upper limit of 4.6×10^{-8} on the branching fraction for $\tau^\mp \rightarrow \mu^\pm \mu^\mp \mu^\mp$.

Finally, the ATLAS experiment has searched for $\tau^\mp \rightarrow \mu^\pm \mu^\mp \mu^\mp$ decays using 8 TeV pp collision data corresponding to an integrated luminosity of 20.3 fb^{-1} [48]. The search selects candidate W boson decays using the missing transverse momentum ($\mathbf{p}_T^{\text{miss}}$) and the transverse mass $m_T = \sqrt{2p_T^\tau p_T^{\text{miss}}(1 - \cos \Delta\phi)}$, where $\Delta\phi$ is the angle between \mathbf{p}_T^τ and $\mathbf{p}_T^{\text{miss}}$. Candidate lepton flavour violating decays are defined as those with three muons within 1 GeV of the mass of the τ lepton, and a loose selection is applied based on kinematics

and displacement of the three-muon vertex relative to the collision point. The large multi-jet background is then removed using a boosted decision tree (BDT) and requiring the three-muon mass to be within ± 64 MeV of the τ lepton mass. The optimal BDT selection leaves 0.2 expected background events with an efficiency of 2.3%. No events are observed, leading to a 90% C.L. upper limit of 3.8×10^{-7} on the branching fraction.

2.2 Future limits

Projections of the current analyses are complicated by the prevalence of misidentification backgrounds, which typically require data to model. A conservative estimate scales the background yield by the projected increase in luminosity and cross section. However, further optimisation of the analyses incorporating upgrades to the detectors could improve these results. As an optimistic estimate the background is kept at the current level with a modest 10% loss of acceptance.

An ongoing upgrade to the KEK accelerator and the Belle detector (Belle-II) will ultimately yield a factor of 50 increase in integrated luminosity, with data taking set to begin in 2017. A conservative estimate of the expected $\tau^\mp \rightarrow \mu^\pm \mu^\mp \mu^\mp$ sensitivity can be made by simply scaling the background from 0.13 to 6.5 events and assuming no change in the reconstruction efficiency. This leads to an expected upper limit of 1.0×10^{-9} on the branching fraction (equal to the projected limit from the experiment [49]). Including a more optimistic projection, the ranges of expected limits are $(4.7\text{--}10) \times 10^{-10}$, $(3.6\text{--}4.7) \times 10^{-10}$, and $(5.9\text{--}12) \times 10^{-10}$ on the branching fractions for $\tau^\mp \rightarrow \mu^\pm \mu^\mp \mu^\mp$, $\tau^\mp \rightarrow e^\pm \mu^\mp \mu^\mp$, and $\tau^\mp \rightarrow e^\mp \mu^\mp \mu^\pm$, respectively.

The upgrade of the LHC accelerator and the LHCb detector will produce a data sample corresponding to an integrated luminosity of 50 fb^{-1} [50] at a centre-of-mass energy of 13 TeV. Taking the ratio of 13 TeV to 7 TeV heavy-quark production cross section to be 1.8 [51–54], the τ lepton yield will increase by approximately a factor of 30. Taking into account the higher background cross section, a conservative estimate of the expected limit is 1.1×10^{-8} . A more optimistic estimate assuming the background can be reduced to its current level gives a 90% C.L. upper limit of 1.5×10^{-9} on the $\tau^\mp \rightarrow \mu^\pm \mu^\mp \mu^\mp$ branching fraction.

The ATLAS sensitivity to the high-luminosity LHC will be affected by a high number of overlapping interactions, potentially leading to lower neutrino momentum resolution and lower trigger efficiencies. Assuming the current performance is approximately achieved through detector upgrade and analysis improvements, the expected τ lepton yields can be scaled to 3 ab^{-1} with a factor of 1.6 increase in cross section [55, 56]. Assuming an equal scaling for the background gives 46 expected background events and a 90% C.L. of 8.1×10^{-9} . In the most optimistic scenario, where the background is suppressed to its current level with a modest 10% efficiency loss, the expected 90% C.L. on the $\tau^\mp \rightarrow \mu^\pm \mu^\mp \mu^\mp$ branching fraction is 1.8×10^{-9} .

A future circular collider (FCC) [57] could further improve sensitivity to these processes. A proton-proton collider with $\sqrt{s} = 100$ TeV would have ~ 7 times the cross section for W and Z boson production than the LHC [58]. Assuming a detector with equivalent sensitivity to ATLAS, projecting the conservative and optimistic limits to 3 ab^{-1} of inte-

Experiment	Current	Projected
Belle	2.1×10^{-8}	$(4.7-10) \times 10^{-10}$
BaBar	3.3×10^{-8}	–
FCC-ee	–	$(5-10) \times 10^{-12}$
LHCb	4.6×10^{-8}	$(1.5-11) \times 10^{-9}$
ATLAS	3.8×10^{-7}	$(1.8-8.1) \times 10^{-9}$
FCC-hh	–	$(3-30) \times 10^{-10}$

Table 1. Current and projected 90% C.L. limits on the $\tau^\mp \rightarrow \mu^\pm \mu^\mp \mu^\mp$ branching fraction. The current limits from the LHC experiments utilise only the 8 TeV data, while the projected limits are based on the complete 13 TeV data sets of 3 ab^{-1} for ATLAS and 50 fb^{-1} for LHCb from the high-luminosity run of the LHC.

Experiment	$\tau^\mp \rightarrow e^\pm \mu^\mp \mu^\mp$		$\tau^\mp \rightarrow e^\mp \mu^\mp \mu^\pm$	
	Current	Projected	Current	Projected
Belle	1.7×10^{-8}	$(3.4-5.1) \times 10^{-10}$	2.7×10^{-8}	$(5.9-12) \times 10^{-10}$
BaBar	2.6×10^{-8}	–	3.2×10^{-8}	–
FCC-ee	–	$(5-10) \times 10^{-12}$	–	$(5-10) \times 10^{-12}$

Table 2. Current and projected 90% C.L. limits on the $\tau^\mp \rightarrow e^\pm \mu^\mp \mu^\mp$ and $\tau^\mp \rightarrow e^\mp \mu^\mp \mu^\pm$ branching fractions.

grated luminosity of a 100 TeV collider gives a range of $(3-30) \times 10^{-10}$ for the 90% C.L. on the $\tau^\mp \rightarrow \mu^\pm \mu^\mp \mu^\mp$ branching fraction. Better sensitivity could be achieved by an e^+e^- collider producing 55 ab^{-1} of integrated luminosity on the Z resonance at four interaction points [59]. Such a collider would produce a total of $\sim 6 \times 10^{11}$ τ leptons, and a typical detector could identify rare decays with a high efficiency and low background. Taking an efficiency of (40–80)% and the background to be negligible, 90% C.L. upper limits would range from $(5-10) \times 10^{-12}$ on the branching fractions for all lepton flavour violating τ lepton decays. Given the high potential sensitivity of such a collider, a more careful assessment is warranted.

In summary, the strongest present limits on $\tau^\mp \rightarrow \mu^\pm \mu^\mp \mu^\mp$ come from Belle and will improve by an order of magnitude to $\leq 10^{-9}$ with the expected 50-fold increase in luminosity from SuperKEKB. Constraints from the LHCb and ATLAS experiments could be within a factor of two of these limits. If CMS can provide similar sensitivity, then the combined hadron collider results could exceed the sensitivity of the e^+e^- constraints. Further gains are possible at the LHC if decays of heavy-flavour mesons and W and Z bosons can all be used by the experiments. In the short term, with the 2016 and 2017 data the LHC experiments could overtake the current Belle and BaBar limits. In the far future, a circular e^+e^- collider with a centre-of-mass energy on the Z resonance could further improve constraints by two orders of magnitude. Table 1 summarises the current and projected limits on the $\tau^\mp \rightarrow \mu^\pm \mu^\mp \mu^\mp$ branching fraction, and table 2 shows the equivalent limits for $\tau^\mp \rightarrow e^\pm \mu^\mp \mu^\mp$ and $\tau^\mp \rightarrow e^\mp \mu^\mp \mu^\pm$.

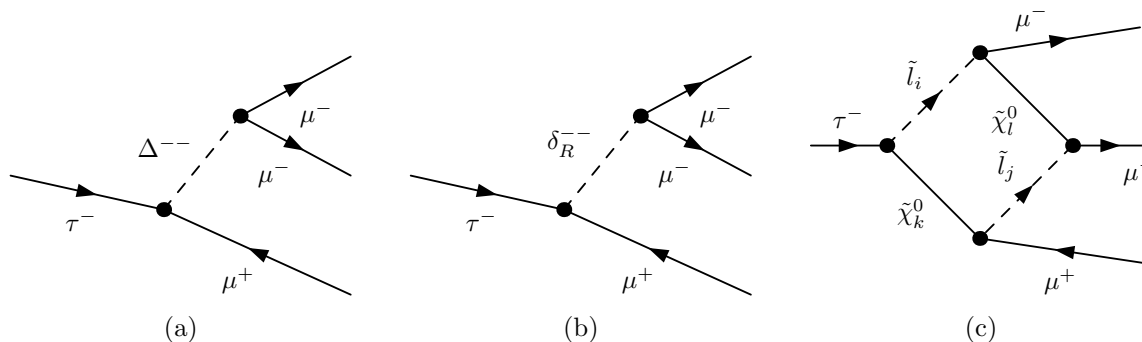


Figure 1. Characteristic Feynman diagrams for the decay $\tau^\mp \rightarrow \mu^\pm \mu^\mp \mu^\mp$ in (a) the Type-II Seesaw Model, (b) the LRSM and (c) the MSSM.

3 Standard Model extensions with lepton flavour violating interactions

Following the effective field theory (EFT) approach, lepton flavour violating interactions $l_i \rightarrow l_j l_k l_l$ can be induced via the dimension-6 operators $\hat{\mathcal{O}}_6 = c_{ijkl} l_i l_j l_k l_l / \Lambda^2$. These LFV operators are generated from the high-scale BSM theories once the heavy particles of the BSM theory are integrated out. As the prototype examples, in the following subsections we consider three BSM extensions: the Type-II Seesaw Model, the Left-Right Symmetric Model and the Minimal Supersymmetric Standard Model. It is worth noting that the chosen seesaw models can generate large LFV rates $l_i \rightarrow l_j l_k l_l$ at tree-level and hence can be highly constrained by the present and future LFV searches. For the MSSM, large flavour violation arises at a loop-induced level. An example Feynman diagram for the process $\tau^\mp \rightarrow \mu^\pm \mu^\mp \mu^\mp$ for each model is shown in figure 1. For the computations of the branching ratios in the Type-II Seesaw Model and the LRSM, we use the program `MadGraph5_aMC@NLO` [60] with the model files generated by `FeynRules` [61]. For the loop-induced decays in the MSSM, we use the spectrum generator `SPheno` [62, 63], with the source code for the flavour observables produced by `SARAH` [64]. We note that the BSM particles that produce this indirect signature could also be directly produced at colliders. For a recent discussion on the collider studies of the seesaw models, see [65–87].

3.1 Type-II Seesaw Model

The model consists of the SM Higgs doublet Φ supplemented by an additional Higgs triplet Δ with hypercharge $Y = +2$,

$$\Phi = \begin{pmatrix} \Phi^+ \\ \Phi^0 \end{pmatrix}, \quad \Delta = \begin{pmatrix} \frac{\Delta^+}{\sqrt{2}} & \Delta^{++} \\ \Delta^0 & -\frac{\Delta^+}{\sqrt{2}} \end{pmatrix}. \quad (3.1)$$

The neutral component Δ^0 has the vacuum expectation value (vev) v_Δ , and generates the Majorana masses of the light neutrinos M_ν . The interaction of Δ with the two lepton doublets is given by,

$$\mathcal{L}_Y(\Phi, \Delta) = Y_\Delta \bar{L}_L^c i \tau_2 \Delta L_L + \text{h.c.} \quad (3.2)$$

Here, c denotes the charge conjugation transformation $\tilde{\Phi} = i\sigma_2\Phi^*$, while Y_Δ is the Yukawa matrix. The light neutrino mass matrix is proportional to the vev v_Δ , with

$$M_\nu = \sqrt{2}Y_\Delta v_\Delta, \quad (3.3)$$

where the triplet vev v_Δ is $v_\Delta = \mu_\Delta v_\Phi^2/(\sqrt{2}M_\Delta^2)$, and v_Φ is the electroweak vev. We note that an equivalent description of the Type-II seesaw is with the triplet Higgs field Δ that gets integrated out and generates the dimension-5 operator $L_i L_j H H/\Lambda$ with the coefficient $C_{ij} = Y_\Delta \mu_\Delta/M_\Delta^2$. The Yukawa Lagrangian generates the following interaction terms between the doubly charged Higgs field Δ^{++} and the pairs of leptons (μ, τ) and (μ, μ) :

$$\mathcal{L}_Y(\Delta^{++}) = Y_{\mu\tau}\bar{\mu}^c\tau\Delta^{++} + Y_{\mu\mu}\bar{\mu}^c\mu\Delta^{++} + \text{h.c.} \quad (3.4)$$

In addition to the Yukawa Lagrangian, the Higgs triplet Δ interacts with the SM Higgs and gauge bosons through the scalar potential and the kinetic Lagrangian. For a complete description of the scalar potential and the other interactions, see [88]. The trilinear interaction of the Δ with the SM Higgs doublet is governed by the following Lagrangian:

$$V(\Phi, \Delta) = \mu_\Delta \Phi^T i\tau_2 \Delta^\dagger \Phi + \text{h.c.} \quad (3.5)$$

The Higgs triplet Δ carries lepton number +2. The simultaneous presence of Y_Δ and μ_Δ gives rise to lepton number violation in this model, while the off-diagonal elements in Y_Δ give rise to flavour violation.

The interaction of the doubly charged Higgs with the two charged leptons gives rise to the lepton flavour violating Higgs decays $l_i \rightarrow l_j l_k l_l$. The partial decay width for $\tau^\mp \rightarrow \mu^\pm \mu^\mp \mu^\mp$ is given by [89],

$$\Gamma(\tau^\mp \rightarrow \mu^\pm \mu^\mp \mu^\mp) = \frac{m_\tau^5}{192\pi^3} |C_{\tau\mu\mu\mu}|^2, \quad (3.6)$$

where the coefficient $C_{\tau\mu\mu\mu}$ has the following form:

$$C_{\tau\mu\mu\mu} = \frac{Y_{\tau\mu} Y_{\mu\mu}}{m_{\Delta^{++}}^2} = \frac{M_\nu(\tau, \mu) M_\nu(\mu, \mu)}{2v_\Delta^2 m_{\Delta^{++}}^2}, \quad (3.7)$$

where $m_{\Delta^{++}}$ is the mass of the doubly charged Higgs and is given by,

$$m_{\Delta^{++}}^2 = M_\Delta^2 - v_\Delta^2 \lambda_3 - \frac{\lambda_4}{2} v_\Phi^2, \quad M_\Delta^2 = \frac{\mu_\Delta v_\Phi^2}{\sqrt{2}v_\Delta}. \quad (3.8)$$

In the above, $\lambda_{3,4}$ are the couplings of the potential [74, 88], and v_Φ is the vev of Φ . The LFV rates for the process $\tau^\mp \rightarrow e^\pm \mu^\mp \mu^\mp$ can be obtained by replacing $M_\nu(\mu, \mu)$ with $M_\nu(e, \mu)$ in eq. (3.6). For detailed discussions on the LFV decays with the other bounds, see [90–93]. Other LFV processes, such as $\mu^\mp \rightarrow e^\pm e^\mp e^\mp$, depend on a different combination of Yukawa couplings and can be suppressed for a large range of neutrino oscillation parameters and phases while still allowing for sizeable LFV τ lepton branching ratios. This was discussed in detail in [90], for both hierarchical and quasi-degenerate neutrino masses, where branching ratios of as large as 10^{-8} for $\tau^\mp \rightarrow \mu^\pm \mu^\mp \mu^\mp$ were obtained, while still being consistent

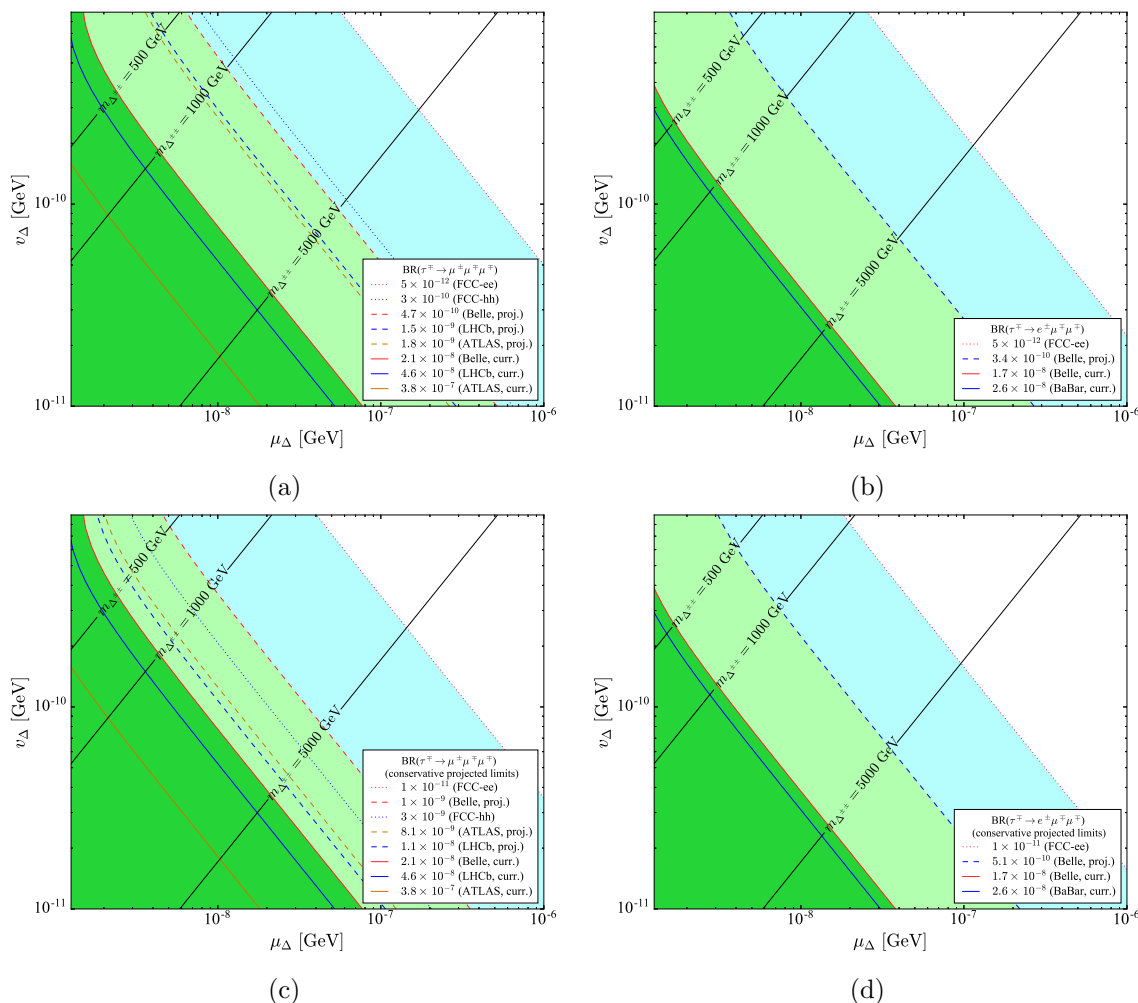


Figure 2. Current and future branching ratio limits in the parameter plane of μ_{Δ} and v_{Δ} for the Type-II Seesaw Model. (a) Shows the limits from the decay $\tau^{\mp} \rightarrow \mu^{\pm} \mu^{\mp} \mu^{\mp}$, and (b) shows the limits from the decay $\tau^{\mp} \rightarrow e^{\pm} \mu^{\mp} \mu^{\mp}$. The same two decay processes are shown in (c) and (d) but with the conservative estimates for the projected limits instead. The solid black lines represent constant values of the mass of the doubly charged Higgs $\Delta^{\pm\pm}$.

with the other bounds. Here we focus on the bounds derived from the LFV τ lepton decays, independent of other constraints. At the end of this subsection, we will give a brief discussion of the consistency of our results with the other bounds when allowing for variations of the neutrino oscillation parameters and phases.

Figure 2 shows the current and future branching ratio limits in the plane of the parameters μ_{Δ} and v_{Δ} , for the two processes $\tau^{\mp} \rightarrow \mu^{\pm} \mu^{\mp} \mu^{\mp}$ and $\tau^{\mp} \rightarrow e^{\pm} \mu^{\mp} \mu^{\mp}$ respectively. We fix the neutrino masses and oscillation parameters to their best-fit values [94, 95] with the lightest neutrino mass at 0.1 eV, and take the PMNS phase to be zero. The solid black lines represent constant values of the doubly charged Higgs mass across the parameter plane. The dark green regions show the parameter space restricted by the current limits, while the pale green regions show the exclusions that can be obtained by projections of

current experiments. Furthermore, the pale blue regions show the restrictions from the future circular colliders FCC-hh and FCC-ee, while the white region is the part of the parameter space that will be allowed by the FCC-ee limit. For the projected limits we show the lower values of the limit ranges in figures 2a and 2b, corresponding to the best possible sensitivity for each experiment. In figures 2c and 2d, we instead show the most conservative estimates for the limits. All other parameter plots in this paper will follow the same scheme for the region colours, and will use the lower values of the limit ranges.

In figure 2, we choose a small v_Δ range, $(10^{-11}-10^{-9})$ GeV, that can naturally explain the small neutrino masses $m_\nu \sim (0.01-0.1)$ eV, with $\mathcal{O}(1)$ coupling. For a moderate $v_\Delta = 10^{-10}$ GeV, and with the neutrino mass $m_\nu \sim 0.1$ eV, the present constraints on μ_Δ and the doubly charged Higgs mass coming from Belle are $\mu_\Delta \geq 7.8 \times 10^{-9}$ GeV and $m_{\Delta\pm\pm} \geq 1.8$ TeV, using the $\tau^\mp \rightarrow \mu^\pm \mu^\mp \mu^\mp$ decay. The future experiments Belle-II and FCC-ee could constrain the doubly charged Higgs mass up to $m_{\Delta\pm\pm} \geq 4.6$ TeV and 14.5 TeV with $\mu_\Delta \geq 5.0 \times 10^{-8}$ GeV and 4.9×10^{-7} GeV, respectively.

The neutrino mass matrix M_ν is diagonalised by the PMNS mixing matrix,

$$U_P^* M_\nu U_P^\dagger = M_d, \tag{3.9}$$

where M_d is the diagonal neutrino mass matrix $M_d = \text{diag}(m_1, m_2, m_3)$, and the PMNS mixing matrix U_P has the following form:

$$U_P = \begin{pmatrix} c_{12}c_{13} & s_{12}c_{13} & s_{13}e^{-i\delta} \\ -c_{23}s_{12} - s_{23}s_{13}c_{12}e^{i\delta} & c_{23}c_{12} - s_{23}s_{13}s_{12}e^{i\delta} & s_{23}c_{13} \\ s_{23}s_{12} - c_{23}s_{13}c_{12}e^{i\delta} & -s_{23}c_{12} - c_{23}s_{13}s_{12}e^{i\delta} & c_{23}c_{13} \end{pmatrix} \begin{pmatrix} 1 & 0 & 0 \\ 0 & e^{i\alpha_1} & 0 \\ 0 & 0 & e^{i\alpha_2} \end{pmatrix}. \tag{3.10}$$

In the above, $s_{ij} \equiv \sin \theta_{ij}$ and $c_{ij} \equiv \cos \theta_{ij}$, where θ_{ij} are the neutrino oscillation parameters. Furthermore, δ is the Dirac CP violating phase and $\alpha_{1,2}$ are the Majorana phases. In figure 3, we allow for a non-zero PMNS phase δ in the range $0-2\pi$, and investigate the effect of varying δ along with the neutrino oscillation parameter θ_{12} on the two decay processes, while fixing the other oscillation parameters to their best-fit values and the lightest neutrino mass to $m_1 = 0.1$ eV. The dark vertical shaded bands show the region of the parameter space allowed by the current 3σ limits on θ_{12} . For the $\tau^\mp \rightarrow \mu^\pm \mu^\mp \mu^\mp$ decay, we consider $\mu_\Delta = 1.5 \times 10^{-7}$ GeV and $v_\Delta = 10^{-10}$ GeV, resulting in $m_{\Delta\pm\pm} = 8.0$ TeV. In the case of $\tau^\mp \rightarrow e^\pm \mu^\mp \mu^\mp$, we use an increased $\mu_\Delta = 2.5 \times 10^{-7}$ GeV and $v_\Delta = 10^{-10}$ GeV, giving $m_{\Delta\pm\pm} = 10.3$ TeV. The Belle-II experiment could rule out δ in the ranges 1.1–2.0 and 4.2–5.1, while experiments at the FCC-ee could exclude all values of δ for these choices of μ_Δ and v_Δ . We find similar constraints when using the $\theta_{23} - \delta$ contours instead, which we do not show here.

We conclude this subsection by justifying our approach of only considering limits from the LFV τ lepton decays. The current bound on the branching fraction for $\mu^\mp \rightarrow e^\pm e^\mp e^\mp$ is $\text{BR}(\mu^\mp \rightarrow e^\pm e^\mp e^\mp) \leq 10^{-12}$ [27]. This tight bound from $\mu^\mp \rightarrow e^\pm e^\mp e^\mp$ imposes stronger limits in the plane of μ_Δ and v_Δ than those arising from the τ lepton decays, shown in figure 2. However, when varying the neutrino oscillation parameters and phases within experimental bounds, it is possible to suppress the branching fraction of $\mu^\mp \rightarrow e^\pm e^\mp e^\mp$

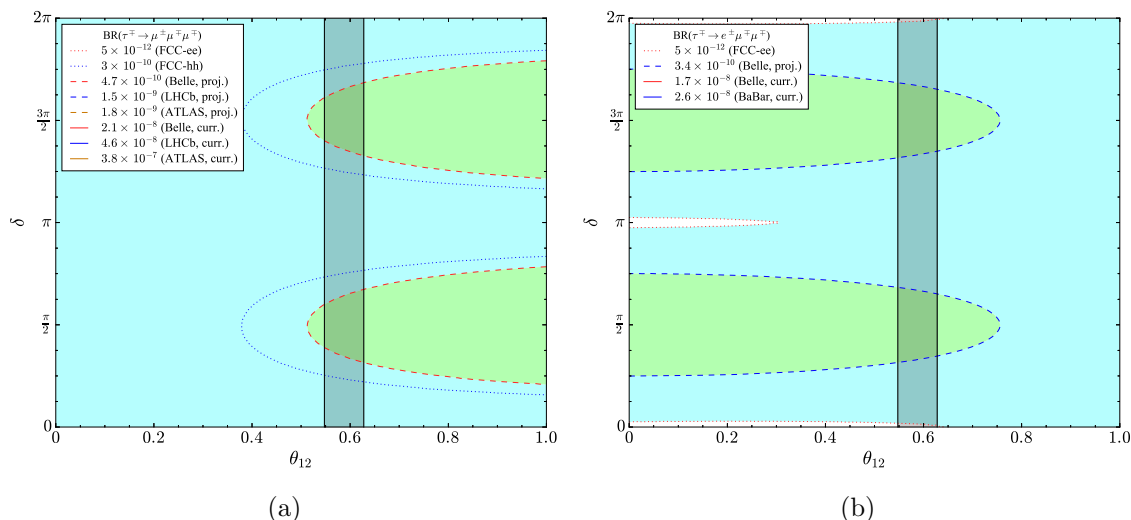


Figure 3. Current and future branching ratio limits in the parameter plane of the neutrino oscillation parameter θ_{12} and the CP violating phase δ for the Type-II Seesaw Model. (a) Shows the limits from the decay $\tau^\mp \rightarrow \mu^\pm \mu^\mp \mu^\mp$, and (b) shows the limits from the decay $\tau^\mp \rightarrow e^\pm \mu^\mp \mu^\mp$. The dark shaded bands represent the allowed 3σ values of θ_{12} .

while leaving that of $\tau \rightarrow \ell \mu \mu$ essentially unchanged. We can consider the oscillation effects by defining the ratio,

$$\mathcal{R} = \frac{\text{BR}(\tau^\mp \rightarrow \mu^\pm \mu^\mp \mu^\mp)}{\text{BR}(\mu^\mp \rightarrow e^\pm e^\mp e^\mp)} \propto \frac{|M_\nu(\mu, \tau) M_\nu(\mu, \mu)|^2}{|M_\nu(\mu, e) M_\nu(e, e)|^2}, \quad (3.11)$$

and varying all the oscillation parameters and phases within their allowed 3σ ranges. For quasi-degenerate neutrino masses with an inverted hierarchy spectrum, and with $m_3 = 0.1 \text{ eV}$, we find that \mathcal{R} can be as large as 10^6 , due to cancellations in the neutrino mass matrix M_ν , which is calculated via eq. (3.9). Such regions of the parameter space suppress the branching ratio of $\mu^\mp \rightarrow e^\pm e^\mp e^\mp$ enough so that the strongest limits on μ_Δ and v_Δ arise from the LFV τ lepton decays, which can remain largely unaffected. Therefore, figure 2 qualitatively demonstrates the constraints that can be obtained in regions where the LFV τ lepton decays provide the dominant source of all LFV decays.

3.2 Left-Right Symmetric Model

The minimal Left-Right Symmetric Model is based on the gauge group $SU(3)_c \times SU(2)_L \times SU(2)_R \times U(1)_{B-L}$ [16–19]. The fermions are assigned in the doublet representations of $SU(2)_L$ and $SU(2)_R$. In addition to the particle content of the Standard Model, the model contains three right-handed Majorana neutrinos N_R paired with the charged leptons l_R , and the additional gauge bosons W_R and Z' . The Higgs fields correspond to a bi-doublet Φ and two Higgs triplets Δ_L and Δ_R with the following quantum numbers under the gauge group: $\Phi(1, 2, 2, 0)$, $\Delta_L(1, 3, 1, 2)$ and $\Delta_R(1, 1, 3, 2)$. The Higgs triplet Δ_R takes the vacuum expectation value v_R and spontaneously breaks $SU(2)_R \times U(1)_{B-L}$ down to the group $U(1)_Y$ of the SM. This generates the masses of the W_R and Z' gauge bosons and

the masses of the right-handed neutrinos. The neutral components of the bi-doublet field Φ also acquire a vev, which is denoted as $\langle \Phi \rangle = \text{diag}(\kappa_1, \kappa_2)/\sqrt{2}$, and this breaks the electroweak symmetry down to $U(1)_Q$, giving masses to the quarks and leptons.

The Higgs triplet Δ_R couples to the right-handed neutrinos N_R and generates the Majorana masses of the heavy neutrinos during the symmetry breaking. The light neutrino masses are generated as a sum of two seesaw contributions, one suppressed by the right-handed neutrino mass (Type-I) [1–5] and the other suppressed by the Higgs triplet mass (Type-II) [6, 7]. The different vevs of the bi-doublets and triplets follow the hierarchy $v_L \ll \kappa_{1,2} \ll v_R$. Below, we discuss the different neutrino masses and the Higgs sector of the LRSM in detail, and their contribution to the tree-level LFV processes $\tau^\mp \rightarrow \mu^\pm \mu^\mp \mu^\mp$ and $\tau^\mp \rightarrow e^\pm \mu^\mp \mu^\mp$.

3.2.1 Neutrino mass

The Yukawa Lagrangian in the lepton sector has the following form:

$$\begin{aligned}
 -\mathcal{L}_Y &= h\bar{\psi}_L\Phi\psi_R + \tilde{h}\bar{\psi}_L\tilde{\Phi}\psi_R + f_L\psi_L^T C i\tau_2 \Delta_L\psi_L \\
 &+ f_R\psi_R^T C i\tau_2 \Delta_R\psi_R + \text{h.c.},
 \end{aligned}
 \tag{3.12}$$

where C is the charge-conjugation matrix, $C = i\gamma_2\gamma_0$, and $\tilde{\Phi} = \tau_2\Phi^*\tau_2$, with τ_2 being the second Pauli matrix. Furthermore, h, \tilde{h}, f_L and f_R are the Yukawa couplings. After symmetry breaking, the Yukawa Lagrangian generates the neutrino mass matrix,

$$\mathcal{M}_\nu = \begin{pmatrix} M_L & M_D \\ M_D^T & M_R \end{pmatrix}.
 \tag{3.13}$$

In the seesaw approximation, this leads to the following light and heavy neutrino mass matrices (up to $\mathcal{O}(M_R^{-1})$) [96]:

$$M_\nu \approx M_L - M_D M_R^{-1} M_D^T = \sqrt{2}v_L f_L - \frac{\kappa^2}{\sqrt{2}v_R} h_D f_R^{-1} h_D^T,
 \tag{3.14}$$

and

$$M_R = \sqrt{2}v_R f_R,
 \tag{3.15}$$

where $\kappa = \sqrt{\kappa_1^2 + \kappa_2^2}$, $M_L = \sqrt{2}v_L f_L$ and the Dirac mass is $M_D = h_D \kappa = (\kappa_1 h + \kappa_2 \tilde{h})/\sqrt{2}$. The mass matrix given in eq. (3.13) can be diagonalised by a 6×6 unitary matrix as follows:

$$\mathcal{V}^T \mathcal{M}_\nu \mathcal{V} = \begin{pmatrix} \tilde{M}_\nu & \mathbf{0} \\ \mathbf{0} & \tilde{M}_R \end{pmatrix},
 \tag{3.16}$$

where $\tilde{M}_\nu = \text{diag}(m_1, m_2, m_3)$ and $\tilde{M}_R = \text{diag}(m_{N_4}, m_{N_5}, m_{N_6})$. In the subsequent analysis, we denote the mixing matrix as,

$$\mathcal{V} = \begin{pmatrix} U & S \\ T & V \end{pmatrix}.
 \tag{3.17}$$

The Yukawa interaction of the doubly charged Higgs with the two charged leptons that mediates the LFV processes $\tau^\mp \rightarrow \mu^\pm \mu^\mp \mu^\mp$ and $\tau^\mp \rightarrow e^\pm \mu^\mp \mu^\mp$ is given by,

$$\mathcal{L}_Y = f_L \bar{l}_L^c \delta_L^{++} l_L + f_R \bar{l}_R^c \delta_R^{++} l_R + \text{h.c.} \quad (3.18)$$

We note that imposing the discrete parity or charge conjugation as a symmetry along with $SU(2)_R \times U(1)_{B-L}$ will lead to $f_L = f_R$ or $f_L = f_R^*$, and a hermitian or symmetric M_D , respectively. As we will show in the next subsection, among the two Higgs triplets $\delta_L^{\pm\pm}$ and $\delta_R^{\pm\pm}$, the right-handed triplet gives the dominant contribution to the tree-level flavour violating processes due to our choice of Higgs masses. Hence, the dominant contribution in the Lagrangian can be approximated as,

$$\mathcal{L}_Y \approx \frac{M_R}{\sqrt{2}v_R} \bar{l}_R^c \delta_R^{++} l_R = \frac{V_R^* \widetilde{M}_R V_R^\dagger}{\sqrt{2}v_R} \bar{l}_R^c \delta_R^{++} l_R + \text{h.c.}, \quad (3.19)$$

where V_R is the diagonalising matrix for the heavy neutrino mass matrix M_R , $V_R^T M_R V_R = \widetilde{M}_R$, and $V \sim V_R$ [96]. A detailed discussion on LFV for this model for all other modes can be found in [38, 41].

3.2.2 Higgs mass

We now discuss the scalar potential and Higgs spectrum in detail. The LRSM consists of the two scalar triplets and one bi-doublet field, that after left-right and electroweak symmetry breaking leads to fourteen physical Higgs states. Among them, a few of the neutral Higgs bosons are required to be heavier than several tens of TeV and do not contribute to the tree-level LFV processes. We follow a simplified approach by judiciously choosing the parameter space, where the doubly charged Higgs arising from Δ_R is lighter than the other BSM Higgs states, and hence gives the dominant contribution in the tree-level LFV processes.

The scalar potential for the LRSM has the following form [97–99]:

$$\begin{aligned} V(\Phi, \Delta_L, \Delta_R) = & -\mu_1^2 \text{Tr} [\Phi^\dagger \Phi] - \mu_2^2 \text{Tr} [\Phi^\dagger \tilde{\Phi} + \tilde{\Phi}^\dagger \Phi] - \mu_3^2 \text{Tr} [\Delta_L^\dagger \Delta_L + \Delta_R^\dagger \Delta_R] \\ & + \lambda_1 [\text{Tr} [\Phi^\dagger \Phi]]^2 + \lambda_2 [\text{Tr} [\Phi^\dagger \tilde{\Phi}]]^2 + \lambda_2 [\text{Tr} [\tilde{\Phi}^\dagger \Phi]]^2 \\ & + \lambda_3 \text{Tr} [\Phi^\dagger \tilde{\Phi}] \text{Tr} [\tilde{\Phi}^\dagger \Phi] + \lambda_4 \text{Tr} [\Phi^\dagger \Phi] \text{Tr} [\Phi^\dagger \tilde{\Phi} + \tilde{\Phi}^\dagger \Phi] \\ & + \rho_1 [\text{Tr} [\Delta_L^\dagger \Delta_L]]^2 + \rho_1 [\text{Tr} [\Delta_R^\dagger \Delta_R]]^2 + \rho_3 \text{Tr} [\Delta_L^\dagger \Delta_L] \text{Tr} [\Delta_R^\dagger \Delta_R] \\ & + \rho_2 \text{Tr} [\Delta_L \Delta_L] \text{Tr} [\Delta_L^\dagger \Delta_L^\dagger] + \rho_2 \text{Tr} [\Delta_R \Delta_R] \text{Tr} [\Delta_R^\dagger \Delta_R^\dagger] \\ & + \rho_4 \text{Tr} [\Delta_L \Delta_L] \text{Tr} [\Delta_R^\dagger \Delta_R^\dagger] + \rho_4 \text{Tr} [\Delta_L^\dagger \Delta_L^\dagger] \text{Tr} [\Delta_R \Delta_R] \\ & + \alpha_1 \text{Tr} [\Phi^\dagger \Phi] \text{Tr} [\Delta_L^\dagger \Delta_L + \Delta_R^\dagger \Delta_R] + \alpha_3 \text{Tr} [\Phi \Phi^\dagger \Delta_L \Delta_L^\dagger + \Phi^\dagger \Phi \Delta_R \Delta_R^\dagger] \\ & + \left\{ \alpha_2 e^{i\delta_2} \text{Tr} [\Phi^\dagger \tilde{\Phi}] \text{Tr} [\Delta_L^\dagger \Delta_L] + \alpha_2 e^{i\delta_2} \text{Tr} [\tilde{\Phi}^\dagger \Phi] \text{Tr} [\Delta_R^\dagger \Delta_R] + \text{h.c.} \right\} \\ & + \beta_1 \text{Tr} [\Phi^\dagger \Delta_L^\dagger \Phi \Delta_R + \Delta_R^\dagger \Phi^\dagger \Delta_L \Phi] + \beta_2 \text{Tr} [\Phi^\dagger \Delta_L^\dagger \tilde{\Phi} \Delta_R + \Delta_R^\dagger \tilde{\Phi}^\dagger \Delta_L \Phi] \\ & + \beta_3 \text{Tr} [\tilde{\Phi}^\dagger \Delta_L^\dagger \Phi \Delta_R + \Delta_R^\dagger \Phi^\dagger \Delta_L \tilde{\Phi}]. \end{aligned} \quad (3.20)$$

The model contains 14 physical Higgs states denoted as h , $H_{1,2,3}^0$, $A_{1,2}^0$, H_1^\pm , H_2^\pm , $\delta_L^{\pm\pm}$, and $\delta_R^{\pm\pm}$ with the masses,

$$\begin{aligned}
 m_h^2 &\approx (125 \text{ GeV})^2 \approx 2\kappa_+^2 \left(\lambda_1 + 4 \frac{\kappa_1^2 \kappa_2^2}{\kappa_+^4} (2\lambda_2 + \lambda_3) + 4\lambda_4 \frac{\kappa_1 \kappa_2}{\kappa_+^2} \right), \\
 M_{H_1^0}^2 = M_{A_1^0}^2 &\approx \alpha_3 \frac{v_R^2}{2} \frac{\kappa_+^2}{\kappa_-^2}, & M_{H_3^0}^2 = M_{A_2^0}^2 &\approx (\rho_3 - 2\rho_1) \frac{v_R^2}{2}, & M_{H_2^0}^2 &\approx 2\rho_1 v_R^2, \\
 M_{H_1^\pm}^2 &\approx (\rho_3 - 2\rho_1) \frac{v_R^2}{2} + \alpha_3 \frac{\kappa_-^2}{4}, & M_{\delta_L^{\pm\pm}}^2 &\approx (\rho_3 - 2\rho_1) \frac{v_R^2}{2} + \alpha_3 \frac{\kappa_-^2}{2}, \\
 M_{H_2^\pm}^2 &\approx \alpha_3 \frac{v_R^2}{2} \frac{\kappa_+^2}{\kappa_-^2} + \alpha_3 \frac{\kappa_-^2}{4}, & M_{\delta_R^{\pm\pm}}^2 &\approx 2\rho_2 v_R^2 + \alpha_3 \frac{\kappa_-^2}{2}. & & (3.21)
 \end{aligned}$$

We note that the scalar states H_1^0 and H_3^0 interact with both the up and down quark sectors and hence mediate the $\Delta F = 2$ flavour transitions in the neutral K and B mesons [100–103]. To avoid the flavour-changing neutral Higgs (FCNH) constraints, the neutral Higgs states H_1^0 , H_3^0 and $A_{1,2}^0$ are required to be heavier than 20 TeV [100–103]. We also consider the other neutral Higgs state H_2^0 to be heavy in order to be in agreement with the heavy Higgs searches at the LHC. In the Higgs spectrum, we consider the case where the right-handed doubly charged Higgs boson is somewhat lighter than the other BSM Higgs states and hence significantly contributes to the LFV processes. We consider the following two benchmark scenarios, BP1 and BP2, with a lower and a higher symmetry breaking scale v_R respectively:

- BP1: $\alpha_3 = 18.88$, $v_R = 8.68 \text{ TeV}$,
- BP2: $\alpha_3 = 1.00$, $v_R = 30.00 \text{ TeV}$.

For both of the benchmark scenarios, we consider the right-handed mixing matrix V_R to be non-diagonal with unit entries everywhere. In order for v_R to be less than 10 TeV, the FCNH constraints on the neutral Higgs bosons necessarily require α_3 to be large ($\alpha_3 \sim 8$). Conversely, when α_3 is well within the perturbative limit, the FCNH constraints on the neutral Higgs bosons demand a large value of the symmetry breaking scale v_R [103]. In our analysis we consider the two possibilities, both the large and the natural α_3 , and show the restrictions that can be obtained on the heavy neutrino masses and the ρ_2 parameter.

3.2.3 Limits from the LFV branching ratios

The two doubly charged Higgs states $\delta_L^{\pm\pm}$ and $\delta_R^{\pm\pm}$ mediate the $\tau \rightarrow l_i l_j l_k$ process at tree-level. The amplitude for the LFV process $\tau^\mp \rightarrow \mu^\pm \mu^\mp \mu^\mp$ is proportional to the coefficient $C_{\tau\mu\mu\mu}$, which is defined as,

$$C_{\tau\mu\mu\mu} = \frac{f_{L\tau\mu} f_{L\mu\mu}}{M_{\delta_L^{\pm\pm}}^2} + \frac{f_{R\tau\mu} f_{R\mu\mu}}{M_{\delta_R^{\pm\pm}}^2}. \quad (3.22)$$

Since in our case the chosen parameter $M_{\delta_L^{\pm\pm}}$ is much heavier than $M_{\delta_R^{\pm\pm}}$, the dominant contribution arises due to $\delta_R^{\pm\pm}$,

$$C_{\tau\mu\mu\mu} = \frac{f_{R\tau\mu} f_{R\mu\mu}}{M_{\delta_R^{\pm\pm}}^2} \approx \frac{M_{R\tau\mu} M_{R\mu\mu}}{2v_R^2 M_{\delta_R^{\pm\pm}}^2} = \frac{(V_R^* \widetilde{M}_R V_R^\dagger)_{\tau\mu} (V_R^* \widetilde{M}_R V_R^\dagger)_{\mu\mu}}{2v_R^2 (2\rho_2 v_R^2 + \alpha_3 \frac{\kappa_-^2}{2})}. \quad (3.23)$$

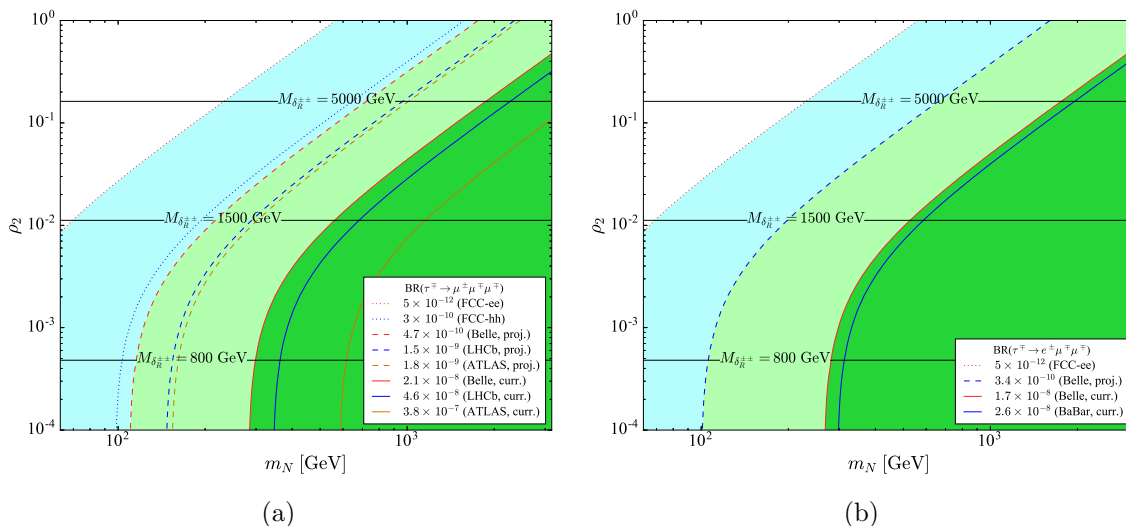


Figure 4. Current and future branching ratio limits in the parameter plane of the right-handed neutrino masses m_N and the parameter ρ_2 for the LRSM for the benchmark scenario BP1. (a) Shows the limits from the decay $\tau^\mp \rightarrow \mu^\pm \mu^\mp \mu^\mp$, and (b) shows the limits from the decay $\tau^\mp \rightarrow e^\pm \mu^\mp \mu^\mp$. The solid black lines represent constant values of the mass of the doubly charged Higgs $\delta_R^{\pm\pm}$.

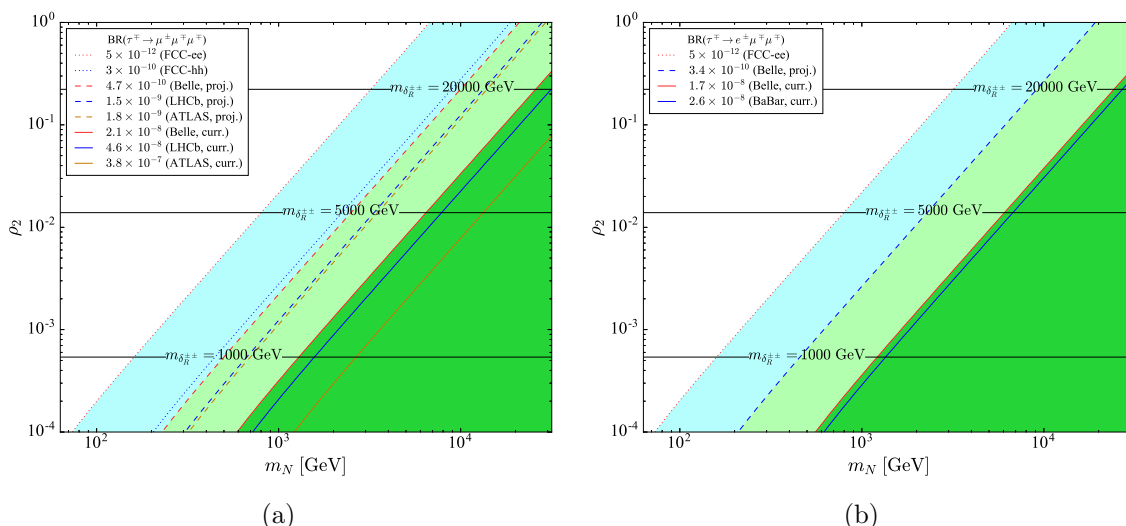


Figure 5. Current and future branching ratio limits in the parameter plane of the right-handed neutrino masses m_N and the parameter ρ_2 for the LRSM for the benchmark scenario BP2. (a) Shows the limits from the decay $\tau^\mp \rightarrow \mu^\pm \mu^\mp \mu^\mp$, and (b) shows the limits from the decay $\tau^\mp \rightarrow e^\pm \mu^\mp \mu^\mp$. The solid black lines represent constant values of the mass of the doubly charged Higgs $\delta_R^{\pm\pm}$.

The amplitude for the LFV process $\tau^\mp \rightarrow e^\pm \mu^\mp \mu^\mp$ can be obtained by replacing the $\tau\mu$ element in eq. (3.23) with the τe element. A limit on the branching ratio of the flavour violating decays will constrain the doubly charged Higgs mass from below and the right-handed neutrino mass from above. In figure 4, corresponding to BP1, we show the branching ratio limits for the case where the three right-handed neutrino masses are all equal and denoted by m_N , and are varied along with the parameter ρ_2 . In figure 5, we show

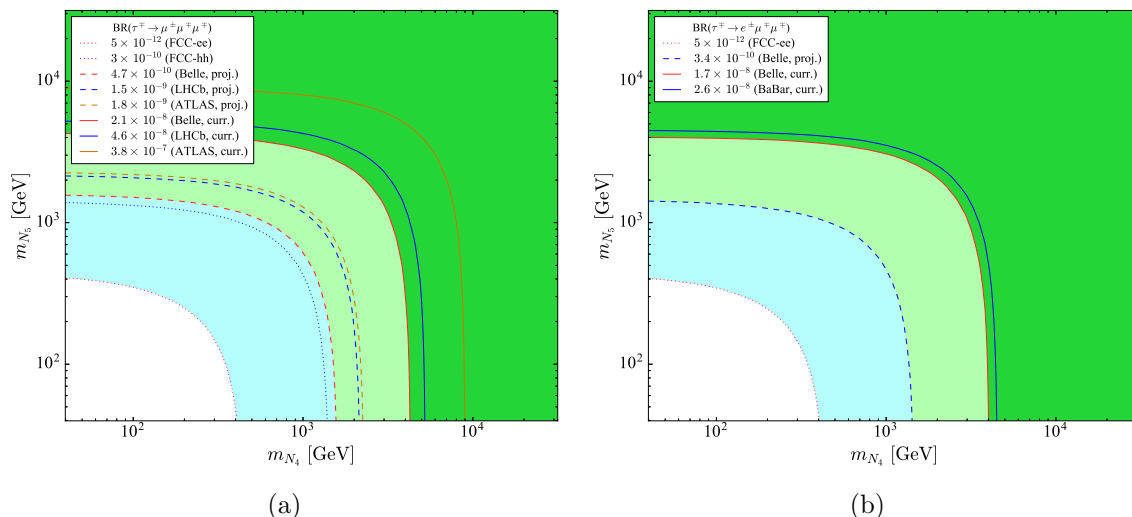


Figure 6. Current and future branching ratio limits in the parameter plane of the right-handed neutrino masses m_{N_4} and m_{N_5} for the LRSM. (a) Shows the limits from the decay $\tau^\pm \rightarrow \mu^\pm \mu^\mp \mu^\mp$, and (b) shows the limits from the decay $\tau^\pm \rightarrow e^\pm \mu^\mp \mu^\mp$.

the equivalent plots for BP2. For BP1, the current limit from Belle imposes the constraint on the right-handed neutrino masses $m_N \leq 290$ GeV for the doubly charged Higgs mass $M_{\delta_R^{\pm\pm}} = 420$ GeV for the $\tau^\pm \rightarrow \mu^\pm \mu^\mp \mu^\mp$ and $\tau^\pm \rightarrow e^\pm \mu^\mp \mu^\mp$ decays. This $M_{\delta_R^{\pm\pm}}$ mass is the lower limit set by the 13 TeV ATLAS search for the right-handed triplet [65]. For BP2, with a higher value of the symmetry breaking scale v_R , the mass limits are much higher: $m_N \lesssim 10$ TeV for the doubly charged Higgs mass $M_{\delta_R^{\pm\pm}} = 8$ TeV. For both of the scenarios, a future circular collider will be able to probe much smaller values of m_N .

In figure 6, we consider the scenario of non-degenerate right-handed neutrino masses $m_{N_{4,5,6}}$. We show the branching ratio limits in the plane of the right-handed neutrino masses m_{N_4} and m_{N_5} for the case of BP1, while fixing $m_{N_6} = 100$ GeV and the doubly charged Higgs mass $M_{\delta_R^{\pm\pm}} = 4$ TeV. The present stringent limit from Belle constrains both of the m_{N_4} and m_{N_5} masses to be smaller than ~ 1 TeV, while the FCC-ee could probe these masses down to ~ 100 GeV.

In our analysis, we considered the possibilities of both a lower and a higher symmetry breaking scale v_R . While a lower symmetry breaking scale and a right-handed gauge boson with mass $M_{W_R} \lesssim (5-6)$ TeV is within the reach of the 13 TeV LHC, a higher symmetry breaking scale, such as that in BP2, along with a much heavier W_R could be probed at a 100 TeV future circular collider [83, 99]. In [99, 104], the impact of renormalisation group evolution of the quartic couplings on the discovery of W_R and the Higgs states has been discussed and bounds on the quartic couplings have been derived by analysing stability conditions. A lower symmetry breaking scale with a W_R accessible at the 13 TeV LHC implies a larger ρ_2 (for a cut-off scale $10M_{W_R}$ with $M_{W_R} = 6$ TeV, then $\rho_2 \geq 0.35$ [99]) and hence a larger $M_{\delta_R^{\pm\pm}}$. This cannot be directly produced at the LHC, but instead can be tested through indirect detection. Conversely, for a larger symmetry breaking scale with $M_{W_R} \sim (20-30)$ TeV the bounds on ρ_2 are relaxed. In our discussion, we do not specify any

particular mass of the other Higgs states and the cut-off scale of the theory. Instead, we independently analyse the implication of the branching ratio limits for the flavour violating processes $\tau^\mp \rightarrow \mu^\pm \mu^\mp \mu^\mp$ and $\tau^\mp \rightarrow e^\pm \mu^\mp \mu^\mp$ on the relevant model parameter ρ_2 and the doubly charged Higgs mass $M_{\delta_R^{\pm\pm}}$.

3.3 Minimal Supersymmetric Standard Model

Within the MSSM the soft supersymmetry breaking parameters in the slepton sector are a generic source of lepton flavour violation. Without assuming a specific SUSY breaking mechanism that ensures a suppression of off-diagonal terms in the slepton mass matrix, their presence can induce a misalignment in flavour space between the lepton and slepton mass matrices, which cannot be rotated away.

The non-diagonal hermitian 6×6 slepton mass matrix receives contributions from D , F , A and M terms [22], where the latter two can induce mixing between different slepton generations. In the electroweak interaction basis $(\tilde{e}_L, \tilde{\mu}_L, \tilde{\tau}_L, \tilde{e}_R, \tilde{\mu}_R, \tilde{\tau}_R)$, the slepton mass matrix has the following form:

$$\mathcal{M}_l^2 = \begin{pmatrix} M_{lLL}^2 & M_{lLR}^2 \\ M_{lLR}^{2\dagger} & M_{lRR}^2 \end{pmatrix}, \tag{3.24}$$

where each of the M_{lLL}^2 , M_{lRR}^2 , M_{lLL}^2 and M_{lLR}^2 is a 3×3 matrix, i.e.

$$\begin{aligned} M_{lLLij}^2 &= m_{Lij}^2 + \left(m_{l_i}^2 + \left(-\frac{1}{2} + \sin^2 \theta_W \right) M_Z^2 \cos 2\beta \right) \delta_{ij}, \\ M_{lRRij}^2 &= m_{Eij}^2 + (m_{l_i}^2 - \sin^2 \theta_W M_Z^2 \cos 2\beta) \delta_{ij}, \\ M_{lLRij}^2 &= v_1 \mathcal{A}_{ij}^l - m_{l_i} \mu \tan \beta \delta_{ij}. \end{aligned} \tag{3.25}$$

In these equations the indices $i, j \in \{1, 2, 3\}$ denote the three generations, m_{l_i} are the lepton masses, θ_W is the weak mixing angle, m_Z is the Z boson mass, $\tan \beta = v_2/v_1$ with $v_1 = \langle H_1 \rangle$ and $v_2 = \langle H_2 \rangle$ being the two vacuum expectation values of the corresponding $SU(2)$ Higgs doublets, and μ is the Higgsino mass term. Here, δ_{ij} is the Kronecker delta symbol. The flavour violating terms in the LL and RR mixing matrices correspond to off-diagonal terms in the soft masses m_{Lij}^2 and m_{Eij}^2 , respectively.

Within the MSSM the sneutrino mass matrix has a one-block 3×3 form denoted as $\mathcal{M}_{\tilde{\nu}}^2$, where in the electroweak basis $(\tilde{\nu}_{eL}, \tilde{\nu}_{\mu L}, \tilde{\nu}_{\tau L})$,

$$\mathcal{M}_{\tilde{\nu}}^2 = M_{\tilde{\nu}LL}^2, \quad M_{\tilde{\nu}LLij}^2 = m_{Lij}^2 + \left(\frac{1}{2} M_Z^2 \cos 2\beta \right) \delta_{ij}. \tag{3.26}$$

To parametrise the off-diagonal entries, we introduce the dimensionless real parameters,

$$\delta_{ij}^{AB} \equiv \frac{M_{lABij}^2}{m_{\tilde{A}_i} m_{\tilde{B}_j}}, \tag{3.27}$$

where $m_{\tilde{L}_i}$ and $m_{\tilde{E}_i}$ are the soft mass scales. We further assume that $|\delta_{ij}^{AB}| \leq 1$, and the hermiticity of \mathcal{M}_l^2 implies $\delta_{ij}^{AB} = \delta_{ji}^{BA}$. After rotating the sleptons and sneutrinos into their

mass eigenstates,

$$\begin{aligned} \text{diag}\{m_{\tilde{l}_1}^2, m_{\tilde{l}_2}^2, m_{\tilde{l}_3}^2, m_{\tilde{l}_4}^2, m_{\tilde{l}_5}^2, m_{\tilde{l}_6}^2\} &= R^{\tilde{l}} \mathcal{M}_{\tilde{l}}^2 R^{\tilde{l}\dagger}, \\ \text{diag}\{m_{\tilde{\nu}_1}^2, m_{\tilde{\nu}_2}^2, m_{\tilde{\nu}_3}^2\} &= R^{\tilde{\nu}} \mathcal{M}_{\tilde{\nu}}^2 R^{\tilde{\nu}\dagger}, \end{aligned} \quad (3.28)$$

the soft breaking terms $m_{\tilde{L}ij}^2$, $m_{\tilde{E}ij}^2$ and \mathcal{A}_{ij}^l can induce flavour-changing neutral current interactions, such as that between a lepton, slepton and neutralino, as shown in the Feynman diagram in figure 1c.

To numerically compute the impact of the present and future LFV constraints on the flavour violating parameters δ_{ij}^{LL} and δ_{ij}^{RR} , we work with the following benchmark point for the MSSM parameters that provides a particle spectrum in agreement with the present collider limits:

$$\begin{aligned} \tan\beta &= 10, & \mu &= -100 \text{ GeV}, \\ M_A &= 1000 \text{ GeV}, & M_1 &= 250 \text{ GeV}, \\ M_2 &= 500 \text{ GeV}, & M_3 &= 2000 \text{ GeV}, \\ m_{\tilde{L}_i} &= m_{\tilde{E}_j} = 1000 \text{ GeV}, & A_\tau &= 200 \text{ GeV}. \end{aligned} \quad (3.29)$$

We do not specify squark supersymmetry breaking parameters here, as their values are not relevant for the processes we calculate. While searches for squarks and gluinos by ATLAS [105, 106] and CMS [107, 108] have pushed their respective mass limits to already rather large values, limits for slepton masses are still fairly weak [26]. Direct slepton pair production requires the exchange of electroweak gauge bosons and is thus strongly suppressed compared to squark or gluino pair production at hadron colliders. Hence, assuming LFV is realised in nature, much stronger limits on the slepton masses can be obtained indirectly by measuring rare flavour violating lepton decays.

In figures 7a and 7b, we show present and future constraints on the pair $(\delta_{23}^{LL}, \delta_{23}^{RR})$ from the process $\tau^\mp \rightarrow \mu^\mp \mu^\mp \mu^\pm$, and the pair $(\delta_{13}^{LL}, \delta_{13}^{RR})$ from the process $\tau^\mp \rightarrow e^\mp \mu^\mp \mu^\pm$, respectively. In analogy with the squark sector [109], we find that the δ_{13}^{RR} and δ_{23}^{RR} parameters are much less constrained than their LL counterparts. This is because the processes are mediated by flavour violating neutralino interactions. In the gauge-interaction basis, the exchanged particles are the bino (\tilde{B}), wino (\tilde{W}^0) or Higgsino (\tilde{H}_i) particles. The $\tilde{H}_i - l_R - \tilde{l}_L$ interactions are proportional to the lepton's Yukawa coupling y_l and are thus subleading, while $\tilde{B} - l_{R/L} - \tilde{l}_{R/L}$ and $\tilde{W}^0 - l_L - \tilde{l}_L$ interactions occur with the strength of their associated gauge couplings. Therefore, the branching ratios $\tau^\mp \rightarrow \mu^\mp \mu^\mp \mu^\pm$ and $\tau^\mp \rightarrow e^\mp \mu^\mp \mu^\pm$ are amplified for a light wino-type neutralino, i.e. small M_2 , and large δ_{ij}^{LL} .

In figure 8, we show the LFV branching ratio limits where the soft slepton mass scale is allowed to vary along with a single mixing parameter. We vary the slepton mass scale over a wide range. For slepton masses at the current lower bound from direct searches (~ 100 GeV) future experiments could place very strong constraints on LFV parameters. Since the slepton masses are large when the soft slepton mass scales $m_{\tilde{L}_i} = m_{\tilde{E}_j}$ are large, their contribution to LFV processes decouples and the sensitivity to the mixing parameters is reduced.

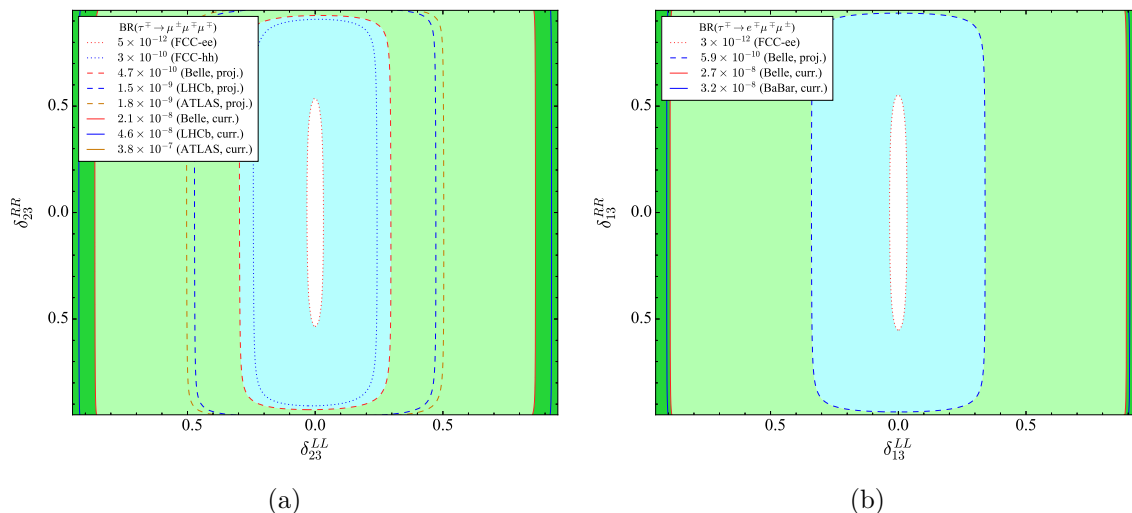


Figure 7. Current and future branching ratio limits in the parameter plane of (a) δ_{23}^{LL} and δ_{23}^{RR} for the decay $\tau^\mp \rightarrow \mu^\pm \mu^\mp \mu^\mp$ and (b) δ_{13}^{LL} and δ_{13}^{RR} for the decay $\tau^\mp \rightarrow e^\mp \mu^\mp \mu^\pm$ in the MSSM.

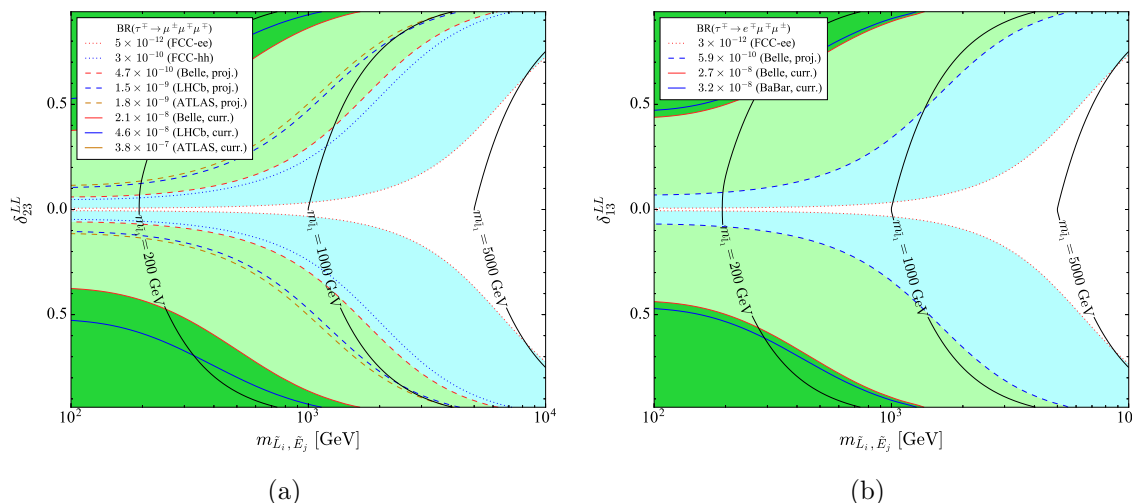


Figure 8. Current and future branching ratio limits in the parameter plane of (a) $m_{\tilde{L}_i, \tilde{E}_j}$ and δ_{23}^{LL} for the decay $\tau^\mp \rightarrow \mu^\pm \mu^\mp \mu^\mp$ and (b) $m_{\tilde{L}_i, \tilde{E}_j}$ and δ_{13}^{LL} for the decay $\tau^\mp \rightarrow e^\mp \mu^\mp \mu^\pm$ in the MSSM. The solid black lines represent constant values of the mass of the slepton \tilde{l}_1 .

4 Conclusions

The experimental observation of lepton flavour violation would unambiguously serve as striking evidence for BSM physics, since in the SM lepton flavour violation is absent to all orders in perturbation theory. A plethora of the ongoing and near future experiments are likely to improve their sensitivity in the τ sector and will probe branching ratios at the level of $\mathcal{O}(10^{-10}-10^{-12})$.

In this work we analyse the flavour violation in the τ sector, with a particular focus on the decays $\tau^\mp \rightarrow \mu^\pm \mu^\mp \mu^\mp$, $\tau^\mp \rightarrow e^\pm \mu^\mp \mu^\mp$ and $\tau^\mp \rightarrow e^\mp \mu^\mp \mu^\pm$ that can arise in various BSM models either at tree-level or with a loop suppression. We review the existing bounds

on the branching ratio limits from Belle, BaBar and the LHC, and summarise the future sensitivity that these could achieve. We also discuss the limits that future circular colliders could reach. In the context of these limits, we provide an analysis of the parameter space that can be restricted in three BSM models that have lepton flavour violating interactions. Our findings are:

- The most stringent limit on the $\tau^\mp \rightarrow \mu^\pm \mu^\mp \mu^\mp$ decay is given by the Belle experiment, with an upper limit on the branching fraction equal to 2.1×10^{-8} at 90% C.L. The LHCb experiment has produced an exclusion limit about two times larger. In the near future the Belle-II experiment will extend sensitivity down to a branching fraction of 4.7×10^{-10} . Although the present limit from ATLAS is an order of magnitude larger than the limit from Belle, the existing and upcoming 13 TeV data sets provide an opportunity for all of the LHC experiments to achieve better sensitivity than Belle. These experiments could produce the strongest limits for several years, until the Belle-II experiment analyses its full data set. The future circular collider FCC-ee could further improve the limits down to 5×10^{-12} , an improvement of almost four orders of magnitude compared to the present bounds. For the $\tau^\mp \rightarrow e^\pm \mu^\mp \mu^\mp$ and $\tau^\mp \rightarrow e^\mp \mu^\mp \mu^\pm$ decays, a similar improvement on the present bounds can be achieved.
- For the Type-II Seesaw Model with a small triplet vev v_Δ in the range $(10^{-11}-10^{-9})$ GeV that naturally explains the $(0.01-1)$ eV light neutrino mass with $\mathcal{O}(1)$ Yukawa coupling Y_Δ , the model parameter μ_Δ is presently constrained as $\mu_\Delta \geq (2 \times 10^{-9}-7 \times 10^{-8})$ GeV. The future circular collider FCC-ee could provide improved constraints on μ_Δ by almost two orders of magnitude. Constraints on the Dirac CP violating phase δ of the PMNS mixing matrix could be obtained by the Belle-II experiment in regions around $\pi/2$ and $3\pi/2$ for a quasi-degenerate neutrino spectrum with the oscillation angles equal to their best-fit values.
- For the LRSM we consider two extreme regimes, with a lower and higher value of the symmetry breaking scale v_R respectively. For the first benchmark point BP1, we consider a somewhat lower $v_R = 8$ TeV and a large $\alpha_3 \sim \mathcal{O}(10)$, and for BP2, we consider a larger $v_R = 30$ TeV with a smaller $\alpha_3 \sim \mathcal{O}(1)$, which is well within the perturbative regime. In BP1, and for a doubly charged Higgs mass $M_{\delta_R^{\pm\pm}} = 800$ GeV, we find that the right-handed neutrino masses $m_N \leq 290$ GeV are in agreement with the present stringent limit from Belle. The future limits from LHCb and Belle-II will further constrain the right-handed neutrino masses down to the $m_N \leq 100$ GeV mass range. Further improvements at the future circular colliders will allow for tighter constraints on the ρ_2 parameter and the doubly charged Higgs mass $M_{\delta_R^{\pm\pm}}$ to be obtained.
- Finally, for the MSSM, we explore the present and future constraints on the dimensionless LFV parameters $\delta_{13}^{LL}, \delta_{23}^{LL}$ (and their RR equivalents) and the soft slepton masses from the $\tau^\mp \rightarrow \mu^\mp \mu^\mp \mu^\pm$ and $\tau^\mp \rightarrow e^\pm \mu^\mp \mu^\mp$ decays. We find that δ_{13}^{LL} and δ_{23}^{LL} are at present bounded by Belle to $|\delta_{13,23}^{LL}| \lesssim 0.9$ for the benchmark scenario we chose. The future constraints from existing colliders will improve the limits to ~ 0.2 , while an FCC-ee collider could further constrain this parameter to as low as 0.03.

Acknowledgments

MS is supported in part by the European Commission through the “HiggsTools” Initial Training Network PITN-GA-2012-316704. MM is supported by the DST-INSPIRE grant INSPIRE-15-0074 and the Royal Society International Exchange Award.

Open Access. This article is distributed under the terms of the Creative Commons Attribution License ([CC-BY 4.0](https://creativecommons.org/licenses/by/4.0/)), which permits any use, distribution and reproduction in any medium, provided the original author(s) and source are credited.

References

- [1] P. Minkowski, $\mu \rightarrow e\gamma$ at a Rate of One Out of 10^9 Muon Decays?, *Phys. Lett.* **B 67** (1977) 421 [[INSPIRE](#)].
- [2] R.N. Mohapatra and G. Senjanović, *Neutrino Mass and Spontaneous Parity Violation*, *Phys. Rev. Lett.* **44** (1980) 912 [[INSPIRE](#)].
- [3] T. Yanagida, *Horizontal Symmetry and Masses of Neutrinos*, *Conf. Proc.* **C7902131** (1979) 95 [[INSPIRE](#)].
- [4] M. Gell-Mann, P. Ramond and R. Slansky, *Complex Spinors and Unified Theories*, *Conf. Proc.* **C 790927** (1979) 315 [[arXiv:1306.4669](#)] [[INSPIRE](#)].
- [5] J. Schechter and J.W.F. Valle, *Neutrino Masses in $SU(2) \times U(1)$ Theories*, *Phys. Rev.* **D 22** (1980) 2227 [[INSPIRE](#)].
- [6] M. Magg and C. Wetterich, *Neutrino Mass Problem and Gauge Hierarchy*, *Phys. Lett.* **B 94** (1980) 61 [[INSPIRE](#)].
- [7] G. Lazarides, Q. Shafi and C. Wetterich, *Proton Lifetime and Fermion Masses in an $SO(10)$ Model*, *Nucl. Phys.* **B 181** (1981) 287 [[INSPIRE](#)].
- [8] T.P. Cheng and L.-F. Li, *Neutrino Masses, Mixings and Oscillations in $SU(2) \times U(1)$ Models of Electroweak Interactions*, *Phys. Rev.* **D 22** (1980) 2860 [[INSPIRE](#)].
- [9] R.N. Mohapatra and G. Senjanović, *Neutrino Masses and Mixings in Gauge Models with Spontaneous Parity Violation*, *Phys. Rev.* **D 23** (1981) 165 [[INSPIRE](#)].
- [10] R. Foot, H. Lew, X.G. He and G.C. Joshi, *Seesaw Neutrino Masses Induced by a Triplet of Leptons*, *Z. Phys.* **C 44** (1989) 441 [[INSPIRE](#)].
- [11] R.N. Mohapatra, *Mechanism for Understanding Small Neutrino Mass in Superstring Theories*, *Phys. Rev. Lett.* **56** (1986) 561 [[INSPIRE](#)].
- [12] R.N. Mohapatra and J.W.F. Valle, *Neutrino Mass and Baryon Number Nonconservation in Superstring Models*, *Phys. Rev.* **D 34** (1986) 1642 [[INSPIRE](#)].
- [13] D. Wyler and L. Wolfenstein, *Massless Neutrinos in Left-Right Symmetric Models*, *Nucl. Phys.* **B 218** (1983) 205 [[INSPIRE](#)].
- [14] E. Witten, *New Issues in Manifolds of $SU(3)$ Holonomy*, *Nucl. Phys.* **B 268** (1986) 79 [[INSPIRE](#)].
- [15] J.L. Hewett and T.G. Rizzo, *Low-Energy Phenomenology of Superstring Inspired E_6 Models*, *Phys. Rept.* **183** (1989) 193 [[INSPIRE](#)].
- [16] J.C. Pati and A. Salam, *Lepton Number as the Fourth Color*, *Phys. Rev.* **D 10** (1974) 275 [*Erratum ibid.* **D 11** (1975) 703] [[INSPIRE](#)].

- [17] R.N. Mohapatra and J.C. Pati, *A Natural Left-Right Symmetry*, *Phys. Rev. D* **11** (1975) 2558 [INSPIRE].
- [18] G. Senjanović and R.N. Mohapatra, *Exact Left-Right Symmetry and Spontaneous Violation of Parity*, *Phys. Rev. D* **12** (1975) 1502 [INSPIRE].
- [19] P. Duka, J. Gluza and M. Zralek, *Quantization and renormalization of the manifest left-right symmetric model of electroweak interactions*, *Annals Phys.* **280** (2000) 336 [hep-ph/9910279] [INSPIRE].
- [20] H.P. Nilles, *Supersymmetry, Supergravity and Particle Physics*, *Phys. Rept.* **110** (1984) 1 [INSPIRE].
- [21] H.E. Haber and G.L. Kane, *The Search for Supersymmetry: Probing Physics Beyond the Standard Model*, *Phys. Rept.* **117** (1985) 75 [INSPIRE].
- [22] S.P. Martin, *A Supersymmetry primer*, hep-ph/9709356 [INSPIRE].
- [23] S. Weinberg, *Baryon and Lepton Nonconserving Processes*, *Phys. Rev. Lett.* **43** (1979) 1566 [INSPIRE].
- [24] F. Wilczek and A. Zee, *Operator Analysis of Nucleon Decay*, *Phys. Rev. Lett.* **43** (1979) 1571 [INSPIRE].
- [25] MEG collaboration, J. Adam et al., *New constraint on the existence of the $\mu^+ \rightarrow e^+ \gamma$ decay*, *Phys. Rev. Lett.* **110** (2013) 201801 [arXiv:1303.0754] [INSPIRE].
- [26] PARTICLE DATA GROUP collaboration, C. Patrignani et al., *Review of Particle Physics*, *Chin. Phys. C* **40** (2016) 100001 [INSPIRE].
- [27] SINDRUM collaboration, U. Bellgardt et al., *Search for the Decay $\mu^+ \rightarrow e^+ e^+ e^-$* , *Nucl. Phys. B* **299** (1988) 1 [INSPIRE].
- [28] CMS collaboration, *Search for Lepton-Flavour-Violating Decays of the Higgs Boson*, *Phys. Lett. B* **749** (2015) 337 [arXiv:1502.07400] [INSPIRE].
- [29] ATLAS collaboration, *Search for lepton-flavour-violating $H \rightarrow \mu\tau$ decays of the Higgs boson with the ATLAS detector*, *JHEP* **11** (2015) 211 [arXiv:1508.03372] [INSPIRE].
- [30] B.M. Dassinger, T. Feldmann, T. Mannel and S. Turczyk, *Model-independent analysis of lepton flavour violating tau decays*, *JHEP* **10** (2007) 039 [arXiv:0707.0988] [INSPIRE].
- [31] R. Harnik, J. Kopp and J. Zupan, *Flavor Violating Higgs Decays*, *JHEP* **03** (2013) 026 [arXiv:1209.1397] [INSPIRE].
- [32] A. Falkowski, D.M. Straub and A. Vicente, *Vector-like leptons: Higgs decays and collider phenomenology*, *JHEP* **05** (2014) 092 [arXiv:1312.5329] [INSPIRE].
- [33] J. Heeck, M. Holthausen, W. Rodejohann and Y. Shimizu, *Higgs $\rightarrow \mu\tau$ in Abelian and non-Abelian flavor symmetry models*, *Nucl. Phys. B* **896** (2015) 281 [arXiv:1412.3671] [INSPIRE].
- [34] A. Crivellin, G. D'Ambrosio and J. Heeck, *Explaining $h \rightarrow \mu^\pm \tau^\mp$, $B \rightarrow K^* \mu^+ \mu^-$ and $B \rightarrow K \mu^+ \mu^- / B \rightarrow K e^+ e^-$ in a two-Higgs-doublet model with gauged $L_\mu - L_\tau$* , *Phys. Rev. Lett.* **114** (2015) 151801 [arXiv:1501.00993] [INSPIRE].
- [35] S. Banerjee, B. Bhattacharjee, M. Mitra and M. Spannowsky, *The Lepton Flavour Violating Higgs Decays at the HL-LHC and the ILC*, *JHEP* **07** (2016) 059 [arXiv:1603.05952] [INSPIRE].
- [36] I. Chakraborty, A. Datta and A. Kundu, *Lepton flavor violating Higgs boson decay $h \rightarrow \mu\tau$ at the ILC*, *J. Phys. G* **43** (2016) 125001 [arXiv:1603.06681] [INSPIRE].

- [37] M. Hirsch, H.V. Klapdor-Kleingrothaus and O. Panella, *Double beta decay in left-right symmetric models*, *Phys. Lett. B* **374** (1996) 7 [[hep-ph/9602306](#)] [[INSPIRE](#)].
- [38] J. Barry and W. Rodejohann, *Lepton number and flavour violation in TeV-scale left-right symmetric theories with large left-right mixing*, *JHEP* **09** (2013) 153 [[arXiv:1303.6324](#)] [[INSPIRE](#)].
- [39] R.L. Awasthi, M.K. Parida and S. Patra, *Neutrino masses, dominant neutrinoless double beta decay and observable lepton flavor violation in left-right models and SO(10) grand unification with low mass W_R, Z_R bosons*, *JHEP* **08** (2013) 122 [[arXiv:1302.0672](#)] [[INSPIRE](#)].
- [40] G. Bambhaniya, P.S.B. Dev, S. Goswami and M. Mitra, *The Scalar Triplet Contribution to Lepton Flavour Violation and Neutrinoless Double Beta Decay in Left-Right Symmetric Model*, *JHEP* **04** (2016) 046 [[arXiv:1512.00440](#)] [[INSPIRE](#)].
- [41] C. Bonilla, M.E. Krauss, T. Opferkuch and W. Porod, *Perspectives for Detecting Lepton Flavour Violation in Left-Right Symmetric Models*, *JHEP* **03** (2017) 027 [[arXiv:1611.07025](#)] [[INSPIRE](#)].
- [42] E. Arganda, M.J. Herrero and J. Portoles, *Lepton flavour violating semileptonic tau decays in constrained MSSM-seesaw scenarios*, *JHEP* **06** (2008) 079 [[arXiv:0803.2039](#)] [[INSPIRE](#)].
- [43] M. Arana-Catania, S. Heinemeyer and M.J. Herrero, *New Constraints on General Slepton Flavor Mixing*, *Phys. Rev. D* **88** (2013) 015026 [[arXiv:1304.2783](#)] [[INSPIRE](#)].
- [44] M. Arana-Catania, E. Arganda and M.J. Herrero, *Non-decoupling SUSY in LFV Higgs decays: a window to new physics at the LHC*, *JHEP* **09** (2013) 160 [Erratum *ibid.* **10** (2015) 192] [[arXiv:1304.3371](#)] [[INSPIRE](#)].
- [45] K. Hayasaka et al., *Search for Lepton Flavor Violating Tau Decays into Three Leptons with 719 Million Produced $\tau^+\tau^-$ Pairs*, *Phys. Lett. B* **687** (2010) 139 [[arXiv:1001.3221](#)] [[INSPIRE](#)].
- [46] BABAR collaboration, J.P. Lees et al., *Limits on tau Lepton-Flavor Violating Decays in three charged leptons*, *Phys. Rev. D* **81** (2010) 111101 [[arXiv:1002.4550](#)] [[INSPIRE](#)].
- [47] LHCb collaboration, *Search for the lepton flavour violating decay $\tau^- \rightarrow \mu^- \mu^+ \mu^-$* , *JHEP* **02** (2015) 121 [[arXiv:1409.8548](#)] [[INSPIRE](#)].
- [48] ATLAS collaboration, *Probing lepton flavour violation via neutrinoless $\tau \rightarrow 3\mu$ decays with the ATLAS detector*, *Eur. Phys. J. C* **76** (2016) 232 [[arXiv:1601.03567](#)] [[INSPIRE](#)].
- [49] T. Aushev et al., *Physics at Super B Factory*, [arXiv:1002.5012](#) [[INSPIRE](#)].
- [50] LHCb collaboration, *Implications of LHCb measurements and future prospects*, *Eur. Phys. J. C* **73** (2013) 2373 [[arXiv:1208.3355](#)] [[INSPIRE](#)].
- [51] LHCb collaboration, *Measurement of J/ψ production in pp collisions at $\sqrt{s} = 7$ TeV*, *Eur. Phys. J. C* **71** (2011) 1645 [[arXiv:1103.0423](#)] [[INSPIRE](#)].
- [52] LHCb collaboration, *Measurement of forward J/ψ production cross-sections in pp collisions at $\sqrt{s} = 13$ TeV*, *JHEP* **10** (2015) 172 [[arXiv:1509.00771](#)] [[INSPIRE](#)].
- [53] LHCb collaboration, *Prompt charm production in pp collisions at $\sqrt{s} = 7$ TeV*, *Nucl. Phys. B* **871** (2013) 1 [[arXiv:1302.2864](#)] [[INSPIRE](#)].
- [54] LHCb collaboration, *Measurements of prompt charm production cross-sections in pp collisions at $\sqrt{s} = 13$ TeV*, *JHEP* **03** (2016) 159 [Erratum *ibid.* **09** (2016) 013] [[arXiv:1510.01707](#)] [[INSPIRE](#)].

- [55] CMS collaboration, *Measurement of inclusive W and Z boson production cross sections in pp collisions at $\sqrt{s} = 8$ TeV*, *Phys. Rev. Lett.* **112** (2014) 191802 [[arXiv:1402.0923](#)] [[INSPIRE](#)].
- [56] ATLAS collaboration, *Measurement of W^\pm and Z-boson production cross sections in pp collisions at $\sqrt{s} = 13$ TeV with the ATLAS detector*, *Phys. Lett. B* **759** (2016) 601 [[arXiv:1603.09222](#)] [[INSPIRE](#)].
- [57] M. Benedikt and F. Zimmermann, *Future Circular Colliders*, CERN-ACC-2015-164 [[INSPIRE](#)].
- [58] M.L. Mangano et al., *Physics at a 100 TeV pp collider: Standard Model processes*, [arXiv:1607.01831](#) [[INSPIRE](#)].
- [59] D. d'Enterria, *Physics at the FCC-ee*, [arXiv:1602.05043](#) [[INSPIRE](#)].
- [60] J. Alwall et al., *The automated computation of tree-level and next-to-leading order differential cross sections and their matching to parton shower simulations*, *JHEP* **07** (2014) 079 [[arXiv:1405.0301](#)] [[INSPIRE](#)].
- [61] A. Alloul, N.D. Christensen, C. Degrande, C. Duhr and B. Fuks, *FeynRules 2.0 — A complete toolbox for tree-level phenomenology*, *Comput. Phys. Commun.* **185** (2014) 2250 [[arXiv:1310.1921](#)] [[INSPIRE](#)].
- [62] W. Porod, *SPheno, a program for calculating supersymmetric spectra, SUSY particle decays and SUSY particle production at e^+e^- colliders*, *Comput. Phys. Commun.* **153** (2003) 275 [[hep-ph/0301101](#)] [[INSPIRE](#)].
- [63] W. Porod and F. Staub, *SPheno 3.1: Extensions including flavour, CP-phases and models beyond the MSSM*, *Comput. Phys. Commun.* **183** (2012) 2458 [[arXiv:1104.1573](#)] [[INSPIRE](#)].
- [64] F. Staub, *SARAH 4: A tool for (not only SUSY) model builders*, *Comput. Phys. Commun.* **185** (2014) 1773 [[arXiv:1309.7223](#)] [[INSPIRE](#)].
- [65] ATLAS collaboration, *Search for doubly-charged Higgs bosons in same-charge electron pair final states using proton-proton collisions at $\sqrt{s} = 13$ TeV with the ATLAS detector*, *ATLAS-CONF-2016-051*.
- [66] ATLAS collaboration, *Search for heavy Majorana neutrinos with the ATLAS detector in pp collisions at $\sqrt{s} = 8$ TeV*, *JHEP* **07** (2015) 162 [[arXiv:1506.06020](#)] [[INSPIRE](#)].
- [67] CMS collaboration, *Search for heavy neutrinos and W bosons with right-handed couplings in proton-proton collisions at $\sqrt{s} = 8$ TeV*, *Eur. Phys. J. C* **74** (2014) 3149 [[arXiv:1407.3683](#)] [[INSPIRE](#)].
- [68] ATLAS collaboration, *Search for new phenomena in dijet mass and angular distributions from pp collisions at $\sqrt{s} = 13$ TeV with the ATLAS detector*, *Phys. Lett. B* **754** (2016) 302 [[arXiv:1512.01530](#)] [[INSPIRE](#)].
- [69] CMS collaboration, *Search for narrow resonances decaying to dijets in proton-proton collisions at $\sqrt{s} = 13$ TeV*, *Phys. Rev. Lett.* **116** (2016) 071801 [[arXiv:1512.01224](#)] [[INSPIRE](#)].
- [70] F.F. Deppisch, P.S. Bhupal Dev and A. Pilaftsis, *Neutrinos and Collider Physics*, *New J. Phys.* **17** (2015) 075019 [[arXiv:1502.06541](#)] [[INSPIRE](#)].
- [71] K.S. Babu and S. Jana, *Probing Doubly Charged Higgs Bosons at the LHC through Photon Initiated Processes*, *Phys. Rev. D* **95** (2017) 055020 [[arXiv:1612.09224](#)] [[INSPIRE](#)].

- [72] M. Nemevšek, F. Nesti, G. Senjanović and Y. Zhang, *First Limits on Left-Right Symmetry Scale from LHC Data*, *Phys. Rev. D* **83** (2011) 115014 [[arXiv:1103.1627](#)] [[INSPIRE](#)].
- [73] M. Nemevšek, F. Nesti and J.C. Vasquez, *Majorana Higgses at colliders*, [arXiv:1612.06840](#) [[INSPIRE](#)].
- [74] M. Mitra, S. Niyogi and M. Spannowsky, *Type-II Seesaw Model and Multilepton Signatures at Hadron Colliders*, *Phys. Rev. D* **95** (2017) 035042 [[arXiv:1611.09594](#)] [[INSPIRE](#)].
- [75] M. Mitra, R. Ruiz, D.J. Scott and M. Spannowsky, *Neutrino Jets from High-Mass W_R Gauge Bosons in TeV-Scale Left-Right Symmetric Models*, *Phys. Rev. D* **94** (2016) 095016 [[arXiv:1607.03504](#)] [[INSPIRE](#)].
- [76] O. Mattelaer, M. Mitra and R. Ruiz, *Automated Neutrino Jet and Top Jet Predictions at Next-to-Leading-Order with Parton Shower Matching in Effective Left-Right Symmetric Models*, [arXiv:1610.08985](#) [[INSPIRE](#)].
- [77] M. Lindner, F.S. Queiroz, W. Rodejohann and C.E. Yaguna, *Left-Right Symmetry and Lepton Number Violation at the Large Hadron Electron Collider*, *JHEP* **06** (2016) 140 [[arXiv:1604.08596](#)] [[INSPIRE](#)].
- [78] M. Lindner, F.S. Queiroz and W. Rodejohann, *Dilepton bounds on left-right symmetry at the LHC run II and neutrinoless double beta decay*, *Phys. Lett. B* **762** (2016) 190 [[arXiv:1604.07419](#)] [[INSPIRE](#)].
- [79] A. Melfo, M. Nemevšek, F. Nesti, G. Senjanović and Y. Zhang, *Type II Seesaw at LHC: The Roadmap*, *Phys. Rev. D* **85** (2012) 055018 [[arXiv:1108.4416](#)] [[INSPIRE](#)].
- [80] A. Maiezza, M. Nemevšek and F. Nesti, *Lepton Number Violation in Higgs Decay at LHC*, *Phys. Rev. Lett.* **115** (2015) 081802 [[arXiv:1503.06834](#)] [[INSPIRE](#)].
- [81] F. del Aguila and J.A. Aguilar-Saavedra, *Distinguishing seesaw models at LHC with multi-lepton signals*, *Nucl. Phys. B* **813** (2009) 22 [[arXiv:0808.2468](#)] [[INSPIRE](#)].
- [82] A. Atre, T. Han, S. Pascoli and B. Zhang, *The Search for Heavy Majorana Neutrinos*, *JHEP* **05** (2009) 030 [[arXiv:0901.3589](#)] [[INSPIRE](#)].
- [83] P.S.B. Dev, R.N. Mohapatra and Y. Zhang, *Probing the Higgs Sector of the Minimal Left-Right Symmetric Model at Future Hadron Colliders*, *JHEP* **05** (2016) 174 [[arXiv:1602.05947](#)] [[INSPIRE](#)].
- [84] S. Banerjee, P.S.B. Dev, A. Ibarra, T. Mandal and M. Mitra, *Prospects of Heavy Neutrino Searches at Future Lepton Colliders*, *Phys. Rev. D* **92** (2015) 075002 [[arXiv:1503.05491](#)] [[INSPIRE](#)].
- [85] P.S.B. Dev, A. Pilaftsis and U.-k. Yang, *New Production Mechanism for Heavy Neutrinos at the LHC*, *Phys. Rev. Lett.* **112** (2014) 081801 [[arXiv:1308.2209](#)] [[INSPIRE](#)].
- [86] A. Das and N. Okada, *Inverse seesaw neutrino signatures at the LHC and ILC*, *Phys. Rev. D* **88** (2013) 113001 [[arXiv:1207.3734](#)] [[INSPIRE](#)].
- [87] A. Das, P. Konar and S. Majhi, *Production of Heavy neutrino in next-to-leading order QCD at the LHC and beyond*, *JHEP* **06** (2016) 019 [[arXiv:1604.00608](#)] [[INSPIRE](#)].
- [88] A. Arhrib et al., *The Higgs Potential in the Type II Seesaw Model*, *Phys. Rev. D* **84** (2011) 095005 [[arXiv:1105.1925](#)] [[INSPIRE](#)].
- [89] A. Abada, C. Biggio, F. Bonnet, M.B. Gavela and T. Hambye, *Low energy effects of neutrino masses*, *JHEP* **12** (2007) 061 [[arXiv:0707.4058](#)] [[INSPIRE](#)].

- [90] D.N. Dinh and S.T. Petcov, *Lepton Flavor Violating τ Decays in TeV Scale Type I See-Saw and Higgs Triplet Models*, *JHEP* **09** (2013) 086 [[arXiv:1308.4311](#)] [[INSPIRE](#)].
- [91] M. Lindner, M. Platscher and F.S. Queiroz, *A Call for New Physics: The Muon Anomalous Magnetic Moment and Lepton Flavor Violation*, [arXiv:1610.06587](#) [[INSPIRE](#)].
- [92] A.G. Akeroyd, M. Aoki and H. Sugiyama, *Lepton Flavour Violating Decays $\tau \rightarrow \bar{l}l$ and $\mu \rightarrow e\gamma$ in the Higgs Triplet Model*, *Phys. Rev. D* **79** (2009) 113010 [[arXiv:0904.3640](#)] [[INSPIRE](#)].
- [93] J. Chakraborty, P. Ghosh, S. Mondal and T. Srivastava, *Reconciling $(g-2)_\mu$ and charged lepton flavor violating processes through a doubly charged scalar*, *Phys. Rev. D* **93** (2016) 115004 [[arXiv:1512.03581](#)] [[INSPIRE](#)].
- [94] I. Esteban, M.C. Gonzalez-Garcia, M. Maltoni, I. Martinez-Soler and T. Schwetz, *Updated fit to three neutrino mixing: exploring the accelerator-reactor complementarity*, *JHEP* **01** (2017) 087 [[arXiv:1611.01514](#)] [[INSPIRE](#)].
- [95] M.C. Gonzalez-Garcia, M. Maltoni and T. Schwetz, *Global Analyses of Neutrino Oscillation Experiments*, *Nucl. Phys. B* **908** (2016) 199 [[arXiv:1512.06856](#)] [[INSPIRE](#)].
- [96] W. Grimus and L. Lavoura, *The seesaw mechanism at arbitrary order: Disentangling the small scale from the large scale*, *JHEP* **11** (2000) 042 [[hep-ph/0008179](#)] [[INSPIRE](#)].
- [97] N.G. Deshpande, J.F. Gunion, B. Kayser and F.I. Olness, *Left-right symmetric electroweak models with triplet Higgs*, *Phys. Rev. D* **44** (1991) 837 [[INSPIRE](#)].
- [98] A. Roitgrund, G. Eilam and S. Bar-Shalom, *Implementation of the left-right symmetric model in FeynRules*, *Comput. Phys. Commun.* **203** (2016) 18 [[arXiv:1401.3345](#)] [[INSPIRE](#)].
- [99] A. Maiezza, G. Senjanović and J.C. Vasquez, *Higgs Sector of the Left-Right Symmetric Theory*, [arXiv:1612.09146](#) [[INSPIRE](#)].
- [100] Y. Zhang, H. An, X. Ji and R.N. Mohapatra, *General CP-violation in Minimal Left-Right Symmetric Model and Constraints on the Right-Handed Scale*, *Nucl. Phys. B* **802** (2008) 247 [[arXiv:0712.4218](#)] [[INSPIRE](#)].
- [101] A. Maiezza and M. Nemevšek, *Strong P invariance, neutron electric dipole moment and minimal left-right parity at LHC*, *Phys. Rev. D* **90** (2014) 095002 [[arXiv:1407.3678](#)] [[INSPIRE](#)].
- [102] S. Bertolini, A. Maiezza and F. Nesti, *Present and Future K and B Meson Mixing Constraints on TeV Scale Left-Right Symmetry*, *Phys. Rev. D* **89** (2014) 095028 [[arXiv:1403.7112](#)] [[INSPIRE](#)].
- [103] A. Maiezza, M. Nemevšek and F. Nesti, *Perturbativity and mass scales in the minimal left-right symmetric model*, *Phys. Rev. D* **94** (2016) 035008 [[arXiv:1603.00360](#)] [[INSPIRE](#)].
- [104] J. Chakraborty, J. Gluza, T. Jelinski and T. Srivastava, *Theoretical constraints on masses of heavy particles in Left-Right Symmetric Models*, *Phys. Lett. B* **759** (2016) 361 [[arXiv:1604.06987](#)] [[INSPIRE](#)].
- [105] ATLAS collaboration, *Summary of the searches for squarks and gluinos using $\sqrt{s} = 8$ TeV pp collisions with the ATLAS experiment at the LHC*, *JHEP* **10** (2015) 054 [[arXiv:1507.05525](#)] [[INSPIRE](#)].
- [106] ATLAS collaboration, *ATLAS Run 1 searches for direct pair production of third-generation squarks at the Large Hadron Collider*, *Eur. Phys. J. C* **75** (2015) 510 [[arXiv:1506.08616](#)] [[INSPIRE](#)].

- [107] CMS collaboration, *Search for supersymmetry in events with one lepton and multiple jets in proton-proton collisions at $\sqrt{s} = 13$ TeV*, *Phys. Rev. D* **95** (2017) 012011 [[arXiv:1609.09386](#)] [[INSPIRE](#)].
- [108] CMS collaboration, *Inclusive search for supersymmetry using razor variables in pp collisions at $\sqrt{s} = 13$ TeV*, *Phys. Rev. D* **95** (2017) 012003 [[arXiv:1609.07658](#)] [[INSPIRE](#)].
- [109] S. Dittmaier, G. Hiller, T. Plehn and M. Spannowsky, *Charged-Higgs Collider Signals with or without Flavor*, *Phys. Rev. D* **77** (2008) 115001 [[arXiv:0708.0940](#)] [[INSPIRE](#)].